



Contents lists available at ScienceDirect

Journal of Advanced Research

journal homepage: www.elsevier.com/locate/jare

Original Article

Phytochemicals and quaternary phosphonium ionic liquids: Connecting the dots to develop a new class of antimicrobial agents

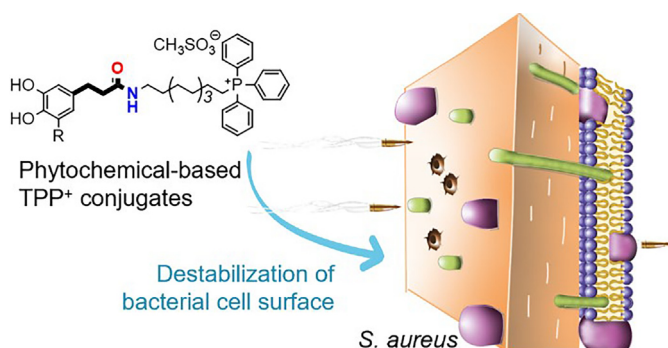
Daniel Chavarria^{a,1}, Anabela Borges^{b,c,1}, Sofia Benfeito^a, Lisa Sequeira^a, Marta Ribeiro^b, Catarina Oliveira^a, Fernanda Borges^{a,*}, Manuel Simões^{b,c,*}, Fernando Cagide^{a,*}

^a CIQUP-IMS/Department of Chemistry and Biochemistry, Faculty of Sciences, University of Porto, Rua do Campo Alegre s/n, 4169-007 Porto, Portugal

^b LEPABE – Laboratory for Process Engineering, Environment, Biotechnology and Energy, Faculty of Engineering, University of Porto, Rua Dr. Roberto Frias, 4200-465 Porto, Portugal

^c ALiCE – Associate Laboratory in Chemical Engineering, Faculty of Engineering, University of Porto, Rua Dr. Roberto Frias, 4200-465 Porto, Portugal

GRAPHICAL ABSTRACT



ARTICLE INFO

Article history:

Received 28 November 2022

Revised 3 February 2023

Accepted 8 February 2023

Available online xxxxx

Keywords:

Antibiotics

Antimicrobial resistance

Phytochemical-based TPP⁺ conjugates

Methicillin-resistant *S. aureus*

Bacterial membrane disruption

ABSTRACT

Introduction: The infections by multidrug-resistant bacteria are a growing threat to human health, and the efficacy of the available antibiotics is gradually decreasing. As such, new antibiotic classes are urgently needed.

Objectives: This study aims to evaluate the antimicrobial activity, safety and mechanism of action of phytochemical-based triphenylphosphonium (TPP⁺) conjugates.

Methods: A library of phytochemical-based TPP⁺ conjugates was repositioned and extended, and its antimicrobial activity was evaluated against a panel of Gram-positive (methicillin-resistant *Staphylococcus aureus* – MRSA) and Gram-negative bacteria (*Escherichia coli*, *Klebsiella pneumoniae*, *Pseudomonas aeruginosa*, *Acinetobacter baumannii*) and fungi (*Candida albicans*, *Cryptococcus neoformans* var. *grubii*). The compounds' cytotoxicity and haemolytic profile were also evaluated. To unravel the mechanism of action of the best compounds, the alterations in the surface charge, bacterial membrane integrity, and cytoplasmic leakage were assessed.

Abbreviations: CAMHB, Cation-adjusted Mueller Hinton broth; CLSI, Clinical & Laboratory Standards Institute; CC₅₀, concentration at 50 % cytotoxicity; DCM, Dichloromethane; DIPEA, *N,N*-diisopropylethylamine; HC₁₀, concentration at 10 % haemolytic activity; HEK293, human embryonic kidney cells; LTA, lipoteichoic acid; MBC, Minimum bactericidal concentration; MIC, minimum inhibitory concentration; MRSA, methicillin-resistant *S. aureus* (MRSA); MTAs, mitochondria-targeted antioxidants; NBS, non-binding surface; OD, optical density; PI, propidium iodide; QAC, quaternary ammonium salts; QPC, quaternary phosphonium salts; RBC, red blood cells; THF, Tetrahydrofuran; TPP, Triphenylphosphine; TPP⁺, Triphenylphosphonium cation; TA, teichoic acid; TLC, thin layer chromatography; VRE, vancomycin-resistant Enterococcus; WTA, wall teichoic acid.

* Corresponding authors at: LEPABE – Laboratory for Process Engineering, Environment, Biotechnology and Energy, Faculty of Engineering, University of Porto, Rua Dr. Roberto Frias, Porto 4200-465, Portugal (M. Simões).

E-mail addresses: mvs@fe.up.pt (M. Simões), fborges@fc.up.pt, fernando.fagin@fc.up.pt (F. Cagide).

¹ These authors contributed equally to this work.

<https://doi.org/10.1016/j.jare.2023.02.004>

2090-1232/© 2023 The Authors. Published by Elsevier B.V. on behalf of Cairo University.

This is an open access article under the CC BY-NC-ND license (<http://creativecommons.org/licenses/by-nc-nd/4.0/>).

Results: Structure-activity-toxicity data revealed the contributions of the different structural components (phenolic ring, carbon-based spacers, carboxamide group, alkyl linker) to the compounds' bioactivity and safety. Dihydrocinnamic derivatives **5 m** and **5 n** stood out as safe, potent and selective antibacterial agents against *S. aureus* (MIC < 0.25 µg/mL; CC₅₀ > 32 µg/mL; HC₁₀ > 32 µg/mL). Mechanistic studies suggest that the antibacterial activity of compounds **5 m** and **5 n** may result from interactions with the bacterial cell wall and membrane.

Conclusions: Collectively, these studies demonstrate the potential of phytochemical-based TPP⁺ conjugates as a new class of antibiotics.

© 2023 The Authors. Published by Elsevier B.V. on behalf of Cairo University. This is an open access article under the CC BY-NC-ND license (<http://creativecommons.org/licenses/by-nc-nd/4.0/>).

Introduction

The discovery and development of antibiotics represents one of the greatest achievements in drug discovery history, being powerful allies in the combat of human infectious diseases [1,2]. Unfortunately, the efficacy of many antibiotics is decreasing at a concerning rate. The misuse and overuse over the last century have been promoting selective pressure on bacteria, leading to the development of resistance to the available antibiotics and posing a serious threat to human health [3,4]. Multidrug-resistant (MDR) bacteria are continuously emerging (e.g.: methicillin-resistant *Staphylococcus aureus* (MRSA), vancomycin-resistant *Enterococcus* (VRE)), and they are difficult to treat as they usually evade the effect of the antibiotics used against them [5].

Infections with drug-resistant bacteria cause approximately 700 000 deaths per year [6,7]. If sufficient attention is not given to this issue, it is estimated that by 2050, infections with MDR pathogenic bacteria will become the leading cause of death [6]. This scenario is further aggravated by the sluggish rate of discovery of new antibiotics, which fail to match the speed of the emergence and spread of MDR bacteria [5]. Moreover, antibiotics own a weak economic turnover, as a result of the scenario of antibiotic resistance coupled with the high costs of bringing a new drug to the market [2,8]. This is one of the main reasons why big pharmaceutical companies have been discontinuing their antimicrobial projects throughout the new millennia [2,8]. Collectively, these factors justify the urgent need of new classes of antibiotics, preferentially with the ability to operate through different mechanisms of action.

Quaternary heteronium salts, such as quaternary ammonium (QAC) and phosphonium compounds (QPCs), are considered a promising inspiration for the discovery of new antibiotics to tackle antibacterial resistance [9]. Quaternary ammonium salts have been used as antiseptics and disinfectants since the 1930's [10] although the exact mechanism of action remains elusive. However, it is well recognized that they can disrupt the structure of the bacterial cytoplasmic membrane affecting its permeability [11,12]. Quaternary phosphonium compounds (QPCs) were discovered in the middle of the 20th century, and their antimicrobial activity and safety in humans has been investigated since then.

The antimicrobial activity of quaternary heteronium salts depends on the density of the cationic charge and the hydrophobicity of the active molecule. Due to the stronger polarization effect of the phosphorus atom compared to the nitrogen atom, QPCs are more readily adsorbed onto the negatively charged bacterial membranes than QACs [13] and usually present higher activity, stability and wider pH applicable range (pH = 2–12) [13].

An important class of QPCs that has been lately developed is triphenylphosphonium (TPP⁺)-based mitochondria-targeted antioxidants (MTAs). They are composed of an antioxidant moiety, usually of natural origin, linked to the mitochondriotropic carrier TPP⁺ through an alkyl spacer [14]. Although TPP⁺-based MTAs have

been widely investigated for their ability to reduce mitochondrial oxidative stress [15], it has been hypothesized that, due to the similar bioenergetic processes between mitochondria and bacteria, they may suppress bacterial growth by uncoupling oxidative phosphorylation [16]. However, the evaluation of the antimicrobial potential of TPP⁺-based MTAs remains poorly explored, with only a handful of studies being published over the last decades. For instance, SKQ1 (Fig. 1), a plastoquinone-based MTA, was proposed as an antimicrobial agent against Gram-positive (*Bacillus subtilis*, *Mycobacterium* sp. and *S. aureus*) and Gram-negative (*Photobacterium phosphoreum* and *Rhodobacter sphaeroides*) bacteria [16,17]. Studies performed in *B. subtilis* indicate that the mechanism of action of SKQ1 may involve a decrease of the bacterial membrane potential [17].

The lack of data related with the antimicrobial activity, mechanism of action, and safety of TPP⁺ conjugates prompted us to conduct this study. Over the last decade, our research group has been developing phytochemical-based TPP⁺ conjugates using natural antioxidants (e.g.: phenolic acids) as inspiration. In general, these compounds exhibited safe cytotoxicity profiles in eukaryotic cell lines [18–21].

Taken in account the growing need of new antibiotics, we decide to repurpose our in-house libraries of TPP⁺-based MTAs (Figs. 1 and 2) and evaluate their antimicrobial activity and safety (cytotoxicity and haemolytic activity) profiles. To establish robust structure-activity-toxicity relationships, we extended our library by synthesizing new TPP⁺ conjugates (Fig. 2). Finally, we selected the most potent compounds to unravel the mechanism of action behind their antimicrobial activity.

Materials and methods

Chemistry

Reagents and general conditions

All reagents were purchased from Sigma-Aldrich and TCI Chemicals. All solvents were *pro analysis* grade from Merck, Carlo Erba Reagents and Scharlab.

Thin layer chromatography (TLC) was performed on precoated silica gel 60 F254 acquired from Merck with layer thickness of 0.2 mm. Reaction control was monitored using ethyl acetate and/or ethyl acetate:methanol (9:1) and spots were visualized under UV detection at 254 and 366 nm. Following the extraction step, the organic layers were dried over anhydrous sodium sulfate. Flash column chromatography was carried out with silica gel 60 0.040–0.063 mm acquired from Carlo-Erba Reactifs. Cellulose flash column chromatography was carried out with cellulose powder 0.01–0.10 mm acquired from Sigma-Aldrich. The elution systems used for flash column chromatography were specified for each compound. The fractions containing the desired product were collected and concentrated under reduced pressure. Solvents were evaporated using a Büchi Rotavapor.

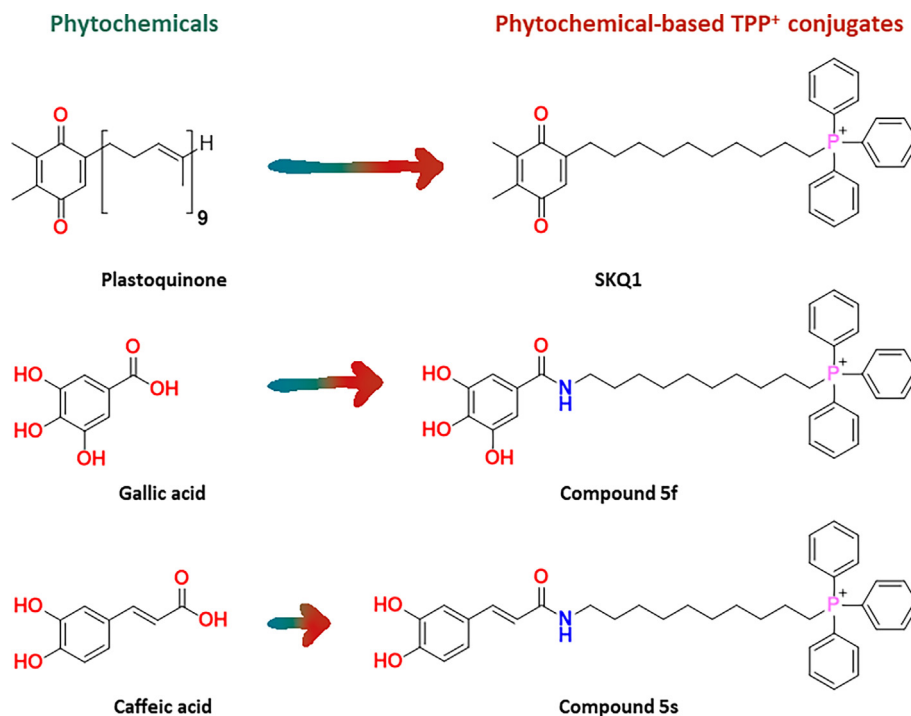


Fig. 1. Examples of phytochemicals and related phytochemical-based TPP⁺ conjugates.

Apparatus

NMR. NMR data were acquired on a Bruker Avance III 400 NMR spectrometer, at room temperature, operating at 400.15 MHz for ¹H and 100.62 MHz for ¹³C and DEPT135 (Distortionless Enhancement by Polarization Transfer). Tetramethylsilane (TMS) was used as internal reference; chemical shifts (δ) were expressed in ppm and coupling constants (J) were given in Hz. DEPT135 values were included in ¹³C NMR data (underline values).

HPLC. Chromatograms were acquired on a Shimadzu high-performance liquid chromatograph (HPLC) SPD-M20A system (Shimadzu, Kyoto, Japan) with a Luna C18 (2) column (Phenomenex, CA, USA) 150x4.6 mm, 5 μ m. The mobile phase was acetonitrile/water (gradient mode, room temperature) at a flow rate of 1 mL/min. The chromatographic data was analysed by the LabSolutions software version 5.93 (Shimadzu, Kyoto, Japan). The purity of the final products (>98%) was verified by high-performance liquid chromatography (HPLC) equipped with a DAD detector (See SI).

Synthesis

General procedure for the synthesis of amides 2a-t, 4u-x and 10a-f

To obtain amides **2a-t**, **4u-x** and **10a-f**, two different synthetic strategies were used. Compounds **2a-b**, **2o-t**, **4u-x** and **10a-f** were synthesized following the procedure **A1**, while compounds **2c-n** were obtained following the procedure **A2**.

Procedure A1. The appropriate carboxylic acid (compounds **1a-b**, **1 g-h** or **9a-c**, Schemes 1-3, 1 mmol) was dissolved in dichloromethane (40 mL), and triethylamine (2 mmol) was added. Then, ethyl chloroformate (2 mmol) was added dropwise to the reaction mixture kept in an ice bath. After stirring for 2 h at room temperature, the appropriate amine (1-amino-6-hexanol, 1-amino-8-octanol, 1-amino-8-octanol, compound **8** or compounds **1i-j**; 2 mmol) was added. The reaction was stirred for 10 h at room temperature. The reaction conditions and work-up were previously described [18,19,21].

Procedure A2. To a solution of the appropriate carboxylic acid (compounds **1a-f**, Scheme 1, 1 mmol) in dichloromethane

(20 mL), phosphorus oxychloride (1 mmol) was added. The reaction mixture was stirred at room temperature for 30 min, then cooled on an ice bath, and the appropriate aminoalkylalcohol (1-amino-6-hexanol, 1-amino-8-octanol or 1-amino-8-octanol; 1.2 mmol) and DIPEA (4 mmol) were added. The reaction mixture was stirred at room temperature for 2 h. The mixture was then extracted, and the combined organic layers were dried over Na₂SO₄, filtered and concentrated. The reaction conditions and work-up were previously described in literature [20,21].

The spectroscopic data of compounds **2a-t** were previously described in literature [18–21].

(8-(2-(3,4-Dimethoxyphenyl)acetamido)octyl)triphenylphosphonium bromide (4u). Procedure A2. η = 65 %. ¹H NMR (CDCl₃): δ = 1.02 – 1.30 (6H, m, (CH₂)₃(CH₂)₃P⁺), 1.30 – 1.45 (2H, m, CH₂(-CH₂)₂P⁺), 1.44 – 1.61 (4H, m, CH₂CH₂P⁺, CH₂(CH₂)₆P⁺), 3.08 (2H, q, J = 6.9 Hz, CH₂(CH₂)₇P⁺), 3.49 (2H, s, CH₂CONH), 3.51 – 3.61 (2H, m, CH₂CH₂P⁺), 3.74 (3H, s, OCH₃), 3.76 (3H, s, OCH₃), 6.69 (1H, d, J = 8.2 Hz, H(5)), 6.82 (1H, dd, J = 8.2, 2.0 Hz, H(6)), 6.90 (1H, d, J = 2.0 Hz, H(2)), 7.59 – 7.78 (15H, m, PPh₃) ¹³C NMR (CDCl₃): 22.4 (d, J_{CP} = 4.7 Hz, CH₂(CH₂)₂P⁺), 22.7 (d, J_{CP} = 50.3 Hz, CH₂P⁺), 26.3 (CH₂(CH₂)₅P⁺), 28.3 (CH₂(CH₂)₄P⁺, CH₂(CH₂)₃P⁺), 28.9 (CH₂(-CH₂)₆P⁺), 29.9 (d, J = 15.8 Hz, CH₂CH₂P⁺), 39.4 (CH₂(CH₂)₇P⁺), 43.1 (CH₂CONH), 56.0 (OCH₃), 56.0 (OCH₃), 111.4 (C(2)), 112.9 (C(5)), 118.3 (d, J_{CP} = 85.9 Hz, 3 \times C(1')), 121.7 (C(6)), 128.8 (C(1')), 130.6 (d, J_{CP} = 12.6 Hz, 3 \times C(3') and 3 \times C(5')), 133.6 (d, J_{CP} = 9.9 Hz, 3 \times C(2') and 3 \times C(6')), 135.2 (d, J_{CP} = 3.0 Hz, 3 \times C(4')), 147.8 (C(4)), 148.9 (C(3)), 171.8 (CO).

(8-(2-(3,4,5-Trimethoxyphenyl)acetamido)octyl)triphenylphosphonium bromide (4v). Procedure A2. η = 69 %. ¹H NMR (CDCl₃): δ = 1.17 – 1.38 (6H, m, (CH₂)₃(CH₂)₃P⁺), 1.45 – 1.55 (2H, m, CH₂(-CH₂)₂P⁺), 1.55 – 1.68 (4H, m, CH₂CH₂P⁺, CH₂(CH₂)₆P⁺), 3.20 (2H, q, J = 6.5 Hz, CH₂(CH₂)₇P⁺), 3.55 – 3.67 (2H, m, CH₂CH₂P⁺), 3.60 (2H, s, CH₂CONH), 3.77 (3H, s, OCH₃), 3.81 (6H, s, 2 \times OCH₃), 6.70 (2H, s, C(2), C(6)), 7.66 – 7.86 (15H, m, PPh₃). ¹³C NMR (CDCl₃): 22.2

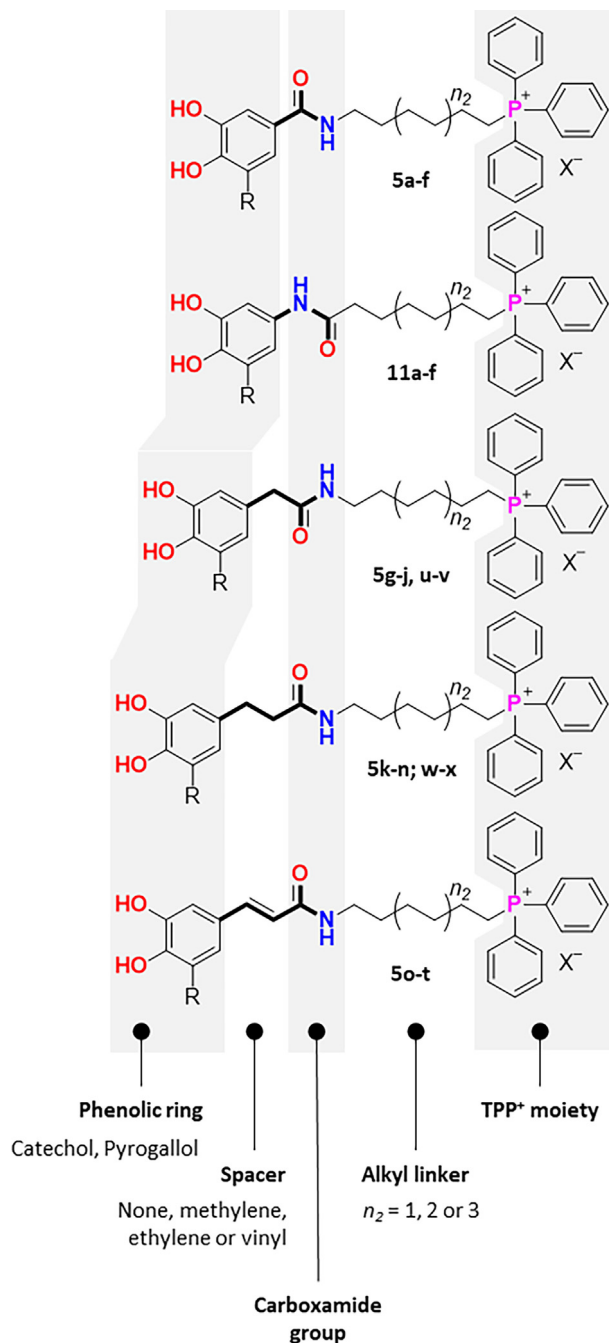


Fig. 2. Rational design strategy followed for the development of phytochemical-based TPP⁺ conjugates.

(d , $J_{CP} = 4.6$ Hz, $\underline{\text{C}}\text{H}_2(\text{CH}_2)_2\text{P}^+$), 22.4 (d , $J_{CP} = 50.4$ Hz, CH_2P^+), 26.1 ($\text{CH}_2(\text{CH}_2)_5\text{P}^+$), 28.1 ($\text{CH}_2(\text{CH}_2)_4\text{P}^+$), 28.2 ($\text{CH}_2(\text{CH}_2)_3\text{P}^+$), 28.9 ($\text{CH}_2(\text{CH}_2)_6\text{P}^+$), 29.7 (d , $J_{CP} = 15.9$ Hz, $\text{CH}_2\text{CH}_2\text{P}^+$), 39.2 ($\text{CH}_2(\text{CH}_2)_7\text{P}^+$), 43.6 (CH_2CONH), 56.1 ($2 \times \text{OCH}_3$), 60.6 (OCH_3), 106.5 ($\text{C}(2)$ and $\text{C}(6)$), 118.6 (d , $J_{CP} = 86.3$ Hz, $3 \times \text{C}(1')$), 130.5 (d , $J_{CP} = 12.4$ Hz, $3 \times \text{C}(3')$ and $3 \times \text{C}(5')$), 132.2 ($\text{C}(1)$), 133.4 (d , $J_{CP} = 10.0$ Hz, $3 \times \text{C}(2')$ and $3 \times \text{C}(6')$), 135.1 (d , $J_{CP} = 3.0$ Hz, $3 \times \text{C}(4')$), 136.2 ($\text{C}(4)$), 152.8 ($\text{C}(3)$ and $\text{C}(5)$), 171.4 (CO).

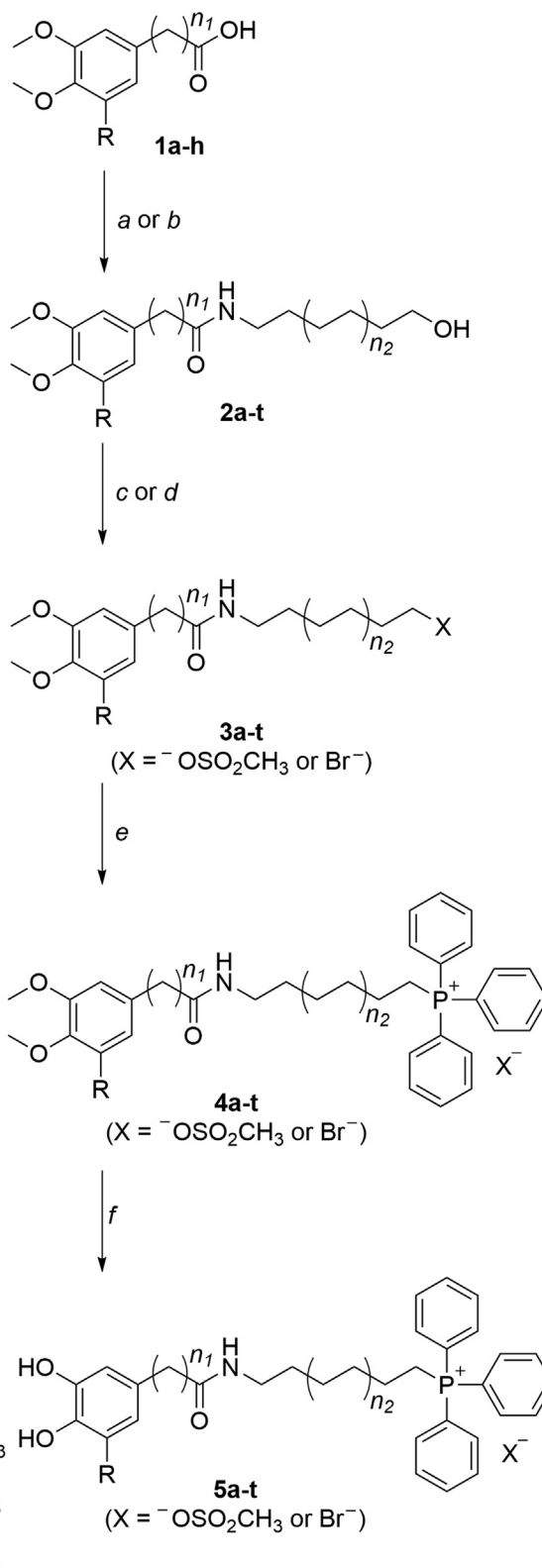
(8-(3-(3,4-Dimethoxyphenyl)propanamido)octyl)triphenylphosphonium bromide (4w). Procedure A2. $\eta = 62\%$. ^1H NMR (MeOD): $\delta = 1.08 - 1.39$ (8H, m, $(\text{CH}_2)_4(\text{CH}_2)_2\text{P}^+$), $1.44 - 1.58$ (2H, m, $\text{CH}_2\text{CH}_2\text{P}^+$), $1.08 - 1.39$ (2H, m, $\text{CH}_2(\text{CH}_2)_6\text{P}^+$), 2.45 (2H, t, $J = 7.4$ Hz,

$\text{CH}_2\text{CH}_2\text{CONH}$), 2.84 (2H, t, $J = 7.4$ Hz, $\text{CH}_2\text{CH}_2\text{CONH}$), $3.34 - 3.46$ (2H, m, CH_2P^+), 3.72 (3H, s, OCH_3), 3.76 (2H, s, OCH_3), 6.73 (1H, dd, $J = 8.2, 2.0$ Hz, H(6)), 6.80 (1H, d, $J = 2.0$ Hz, H(2)), 6.82 (1H, d, $J = 8.4$ Hz, H(5)), $7.71 - 7.93$ (15H, m, PPh_3). ^{13}C NMR (MeOD): 21.3 (d , $J_{CP} = 51.0$ Hz, CH_2P^+), 22.1 (d , $J_{CP} = 4.3$ Hz, $\text{CH}_2(\text{CH}_2)_2\text{P}^+$), 26.2 ($\text{CH}_2(\text{CH}_2)_5\text{P}^+$), 28.3 ($\text{CH}_2(\text{CH}_2)_4\text{P}^+$), 28.6 ($\text{CH}_2(\text{CH}_2)_3\text{P}^+$), 28.8 ($\text{CH}_2(\text{CH}_2)_6\text{P}^+$), 30.1 (d , $J_{CP} = 16.1$ Hz, $\text{CH}_2\text{CH}_2\text{P}^+$), 31.1 ($\text{CH}_2\text{CH}_2\text{CONH}$), 37.6 ($\text{CH}_2\text{CH}_2\text{CONH}$), 38.9 ($\text{CH}_2(\text{CH}_2)_7\text{P}^+$), 55.0 (OCH_3), 55.1 (OCH_3), 111.8 ($\text{C}(5)$), 112.2 ($\text{C}(2)$), 118.6 (d , $J_{CP} = 86.2$ Hz, $3 \times \text{C}(1')$), 120.4, 130.1 (d , $J_{CP} = 12.6$ Hz, $3 \times \text{C}(3')$ and $3 \times \text{C}(5')$), 133.4 (d , $J_{CP} = 10.0$ Hz, $3 \times \text{C}(2')$ and $3 \times \text{C}(6')$), 134.9 (d , $J_{CP} = 3.2 - 3.4$ Hz, $3 \times \text{C}(4')$), 147.6 ($\text{C}(4)$), 149.0 ($\text{C}(3)$), 173.8 (CO).

- 1a. R = H; $n_1 = 0$
 1b. R = OCH₃; $n_1 = 0$
 1c. R = H; $n_1 = 1$
 1d. R = OCH₃; $n_1 = 1$
 1e. R = H; $n_1 = 2$
 1f. R = OCH₃; $n_1 = 2$
 1g. R = H; $n_1 = \text{CH=CH}$
 1h. R = OCH₃; $n_1 = \text{CH=CH}$

- 2a, 3a, 4a. R = H; $n_1 = 0$; $n_2 = 1$
 2b, 3b, 4b. R = OCH₃; $n_1 = 0$; $n_2 = 1$
 2c, 3c, 4c. R = H; $n_1 = 0$; $n_2 = 2$
 2d, 3d, 4d. R = OCH₃; $n_1 = 0$; $n_2 = 2$
 2e, 3e, 4e. R = H; $n_1 = 0$; $n_2 = 3$
 2f, 3f, 4f. R = OCH₃; $n_1 = 0$; $n_2 = 3$
 2g, 3g, 4g. R = H; $n_1 = 1$; $n_2 = 1$
 2h, 3h, 4h. R = OCH₃; $n_1 = 1$; $n_2 = 1$
 2i, 3i, 4i. R = H; $n_1 = 1$; $n_2 = 3$
 2j, 3j, 4j. R = OCH₃; $n_1 = 1$; $n_2 = 3$
 2k, 3k, 4k. R = H; $n_1 = 2$; $n_2 = 1$
 2l, 3l, 4l. R = OCH₃; $n_1 = 2$; $n_2 = 1$
 2m, 3m, 4m. R = H; $n_1 = 2$; $n_2 = 3$
 2n, 3n, 4n. R = OCH₃; $n_1 = 2$; $n_2 = 3$
 2o, 3o, 4o. R = H; $n_1 = \text{CH=CH}$; $n_2 = 1$
 2p, 3p, 4p. R = OCH₃; $n_1 = \text{CH=CH}$; $n_2 = 1$
 2q, 3q, 4q. R = H; $n_1 = \text{CH=CH}$; $n_2 = 2$
 2r, 3r, 4r. R = OCH₃; $n_1 = \text{CH=CH}$; $n_2 = 2$
 2s, 3s, 4s. R = H; $n_1 = \text{CH=CH}$; $n_2 = 3$
 2t, 3t, 4t. R = OCH₃; $n_1 = \text{CH=CH}$; $n_2 = 3$

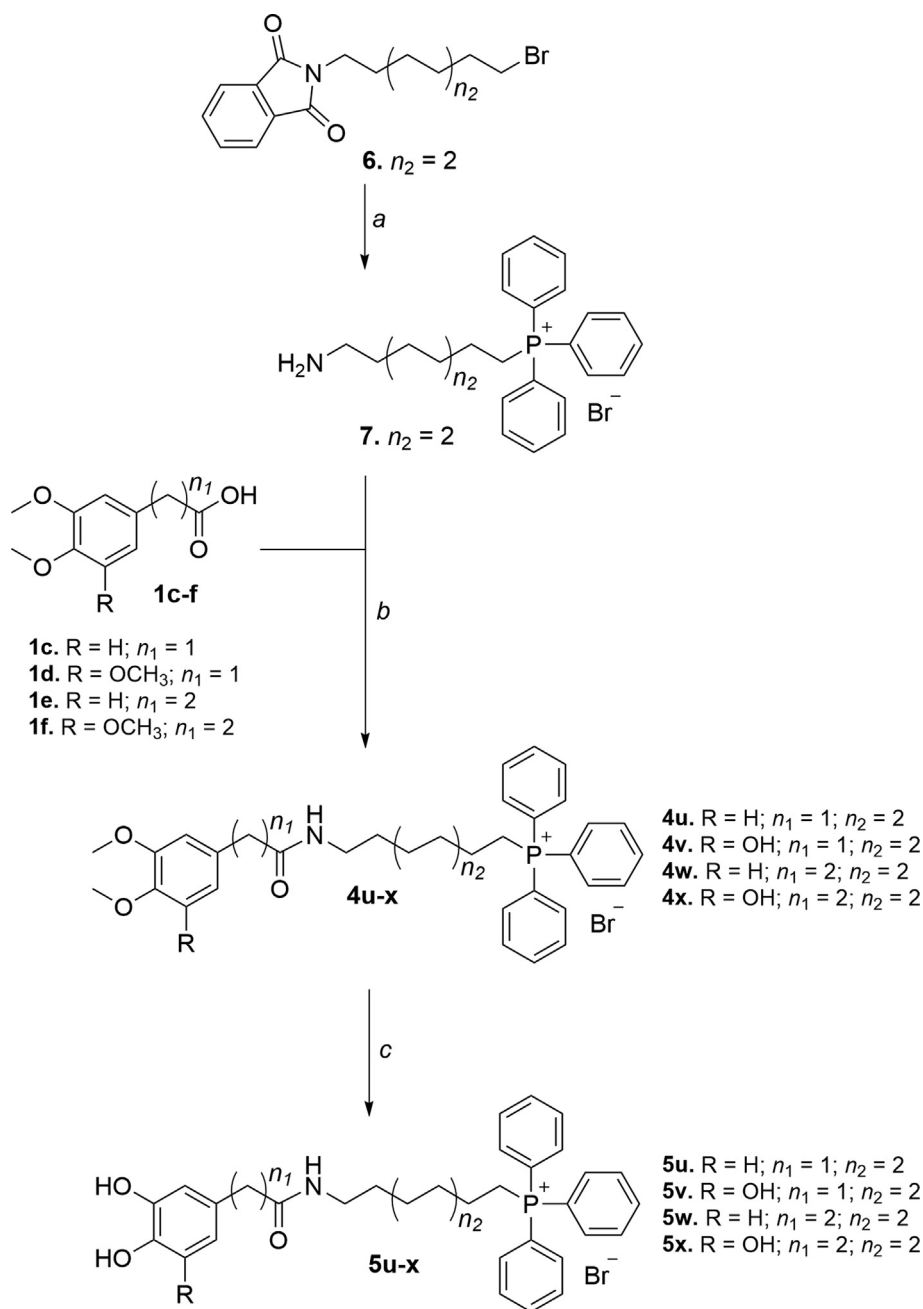
- 5a. R = H; $n_1 = 0$; $n_2 = 1$; X = Br⁻
 5b. R = OH; $n_1 = 0$; $n_2 = 1$; X = Br⁻
 5c. R = H; $n_1 = 0$; $n_2 = 2$; X = Br⁻
 5d. R = OH; $n_1 = 0$; $n_2 = 2$; X = Br⁻
 5e. R = H; $n_1 = 0$; $n_2 = 3$; X = Br⁻
 5f. R = OH; $n_1 = 0$; $n_2 = 3$; X = Br⁻
 5g. R = H; $n_1 = 1$; $n_2 = 1$; X = ⁻OSO₂CH₃
 5h. R = OH; $n_1 = 1$; $n_2 = 1$; X = ⁻OSO₂CH₃
 5i. R = H; $n_1 = 1$; $n_2 = 3$; X = ⁻OSO₂CH₃
 5j. R = OH; $n_1 = 1$; $n_2 = 3$; X = ⁻OSO₂CH₃
 5k. R = H; $n_1 = 2$; $n_2 = 1$; X = ⁻OSO₂CH₃
 5l. R = OH; $n_1 = 2$; $n_2 = 1$; X = ⁻OSO₂CH₃
 5m. R = H; $n_1 = 2$; $n_2 = 3$; X = ⁻OSO₂CH₃
 5n. R = OH; $n_1 = 2$; $n_2 = 3$; X = ⁻OSO₂CH₃
 5o. R = H; $n_1 = \text{CH=CH}$; $n_2 = 1$; X = ⁻OSO₂CH₃
 5p. R = OH; $n_1 = \text{CH=CH}$; $n_2 = 1$; X = ⁻OSO₂CH₃
 5q. R = H; $n_1 = \text{CH=CH}$; $n_2 = 2$; X = ⁻OSO₂CH₃
 5r. R = OH; $n_1 = \text{CH=CH}$; $n_2 = 2$; X = ⁻OSO₂CH₃
 5s. R = H; $n_1 = \text{CH=CH}$; $n_2 = 3$; X = ⁻OSO₂CH₃
 5t. R = OH; $n_1 = \text{CH=CH}$; $n_2 = 3$; X = ⁻OSO₂CH₃



Scheme 1. Synthetic strategy followed to obtain phytochemical-based TPP⁺ conjugates **5a-t**. Reagents and conditions: (a) appropriate hydroxyalkylamines (1-amino-6-hexanol, 1-amino-8-octanol or 1-amino-10-decanol), (C₂H₅)₃N, ClCOOC₂H₅, DCM, r.t., 10 h; (b) POCl₃, DIPEA, DCM, r.t., 1–2 h; (c) C₂Br₂Cl₄, diphos, THF, r.t., 20 h; (d) (C₂H₅)₃N, CH₃SO₂Cl, THF, r.t., 12 h; (e) TPP, 100–130 °C, 48 h; (f) BBr₃, anhydrous DCM, –70 °C to r.t., 12 h.

(8-(3-(3,4,5-Trimethoxyphenyl)propanamido)octyl)triphenyl phosphonium bromide (4x). Procedure A2. $\eta = 65$ %. ¹H NMR (MeOD): $\delta = 1.11 - 1.41$ (6H, m, (CH₂)₃(CH₂)₃P⁺), 1.46 – 1.56 (2H,

m, CH₂(CH₂)₂P⁺), 1.59 – 1.73 (4H, m, CH₂CH₂P⁺, CH₂(CH₂)₆P⁺), 2.48 (2H, t, $J = 7.3$ Hz, CH₂CH₂CONH), 2.85 (2H, t, $J = 7.3$ Hz, CH₂-CH₂CONH), 3.09 (2H, t, $J = 6.9$ Hz, CH₂(CH₂)₇P⁺), 3.32 – 3.45 (2H,

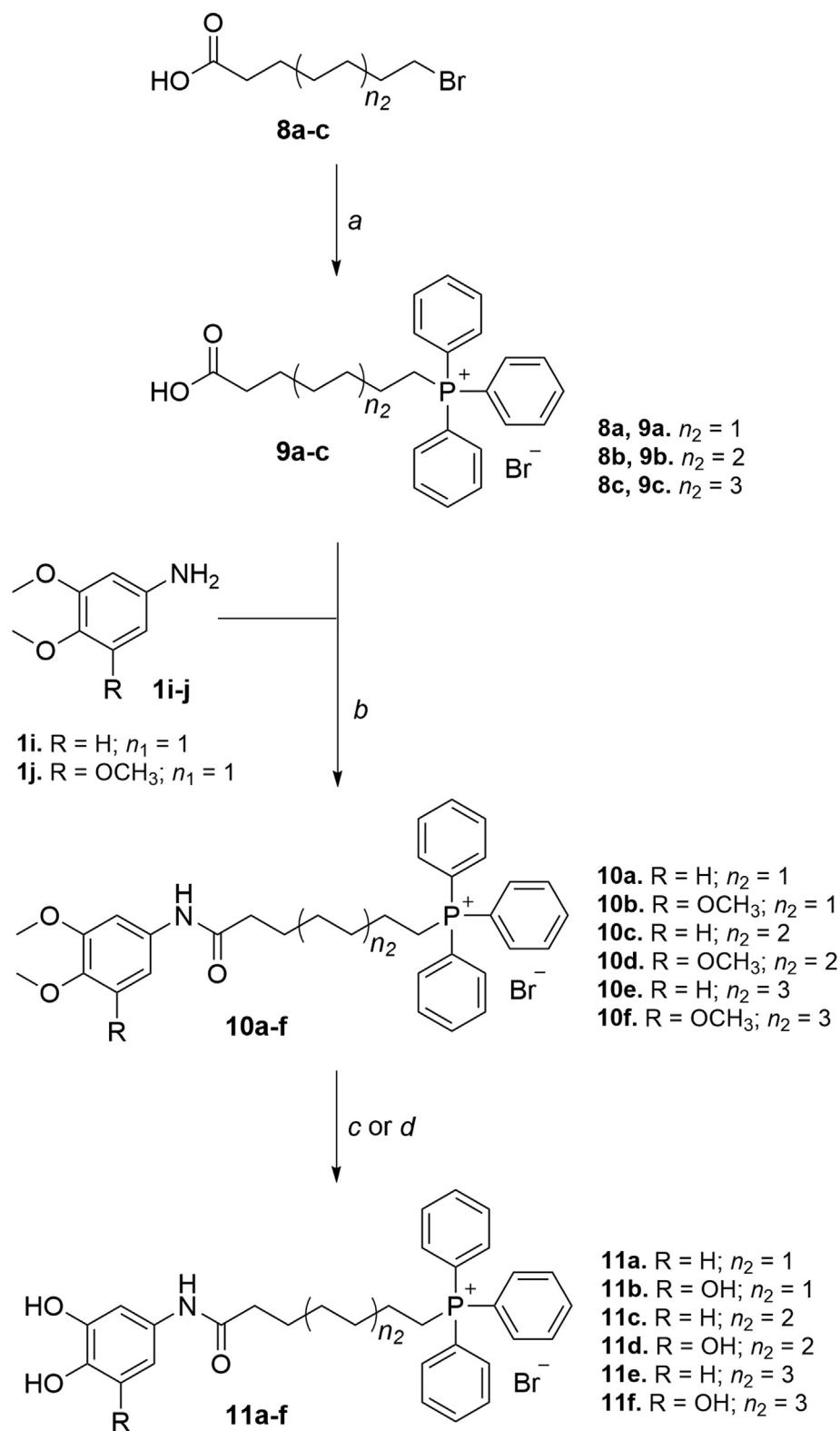


Scheme 2. Synthetic strategy followed to obtain phytochemical-based TPP⁺ conjugates **5u-x**. Reagents and conditions: (a) 1) TPP, 130 °C, 2 h, 2) CH₃(CH₂)₃NH₂, CH₃CH₂OH, reflux, 2 h; (b) (C₂H₅)₃N, ClCOOC₂H₅, DCM, r.t., 10 h; (c) BBr₃, anhydrous DCM, -70 °C to r.t., 12 h.

m, CH₂P⁺), 3.64 (3H, s, OCH₃), 3.79 (6H, s, 2 × OCH₃), 6.51 (2H, s, C(2), C(6)), 7.68 – 7.94 (15H, m, PPh₃). ¹³C NMR (MeOD): 21.3 (d, J_{CP} = 50.9 Hz, CH₂P⁺), 22.1 (d, J_{CP} = 4.5 Hz, CH₂(CH₂)₂P⁺), 26.2 (CH₂(-CH₂)₅P⁺), 28.3 (CH₂(CH₂)₄P⁺), 28.6 (CH₂(CH₂)₃P⁺), 28.9 (CH₂(CH₂)₆-P⁺), 30.1 (d, J_{CP} = 16.1 Hz, CH₂CH₂P⁺), 31.8 (CH₂CH₂CONH), 37.4 (CH₂CH₂CONH), 38.9 (CH₂(CH₂)₇P⁺), 55.2 (2 × OCH₃), 59.7 (OCH₃), 105.4 (C(2) and C(6)), 118.6 (d, J_{CP} = 86.3 Hz, 3 × C(1')), 130.1 (d, J_{CP} = 12.6 Hz, 3 × C(3') and 3 × C(5')), 133.4 (d, J_{CP} = 10.2 Hz, 3 × C(2') and 3 × C(6')), 134.9 (d, J_{CP} = 3.0 Hz, 3 × C(4')), 136.1 (C(1)), 136.8 (C(4)), 153.0 (C(3) and C(5)), 173.7 (CO).

(7-((3,4-Dimethoxyphenyl)amino)-7-oxoheptyl)triphenylphosphonium bromide (10a). Procedure A1. η = 83 %. ¹H NMR (CDCl₃): δ = 1.42 – 1.52 (2H, m, CH₂(CH₂)₂P⁺), 1.54 – 1.65 (2H,

m, CH₂CH₂P⁺), 1.67 – 1.76 (2H, m, CH₂(CH₂)₃P⁺), 1.80 – 1.85 (2H, m, CH₂(CH₂)₄P⁺), 2.63 (2H, t, J = 6.9 Hz, CH₂(CH₂)₅P⁺), 3.62 – 3.73 (2H, m, CH₂P⁺), 3.82 (3H, s, OCH₃), 3.84 (3H, s, OCH₃), 6.71 (1H, d, J = 8.7 Hz, H(5)), 7.51 (1H, dd, J = 2.4, 8.7 Hz, H(6)), 7.58 – 7.78 (15H, m, PPh₃), 7.81 (1H, d, J = 2.4 Hz, H(2)), 10.40 (1H, s, NH). ¹³C NMR (CDCl₃): δ = 22.0 (d, J_{CP} = 4.3 Hz, CH₂(CH₂)₂-P⁺), 22.2 (d, J_{CP} = 50.1 Hz, CH₂P⁺), 24.7 (CH₂(CH₂)₄P⁺), 26.5 (CH₂(-CH₂)₃P⁺), 28.3 (d, J_{CP} = 16.6 Hz, CH₂CH₂P⁺), 36.1 (CH₂(CH₂)₅P⁺), 56.1 (OCH₃), 56.3 (OCH₃), 104.9 (C(2)), 111.3 (C(6)), 111.8 (C(5)), 118.4 (d, J_{CP} = 85.8 Hz, 3 × C(1')), 130.6 (d, J_{CP} = 12.5 Hz, 3 × C(3') and 3 × C(5')), 133.8 (d, J_{CP} = 9.9 Hz, 3 × C(2') and 3 × C(6')), 134.0 (C(1)), 135.1 (d, J_{CP} = 2.9 Hz, 3 × C(4')), 144.8 (C(4)), 148.7 (C(3)), 172.9 (CO).



Scheme 3. Synthetic strategy followed to obtain phytochemical-based TPP⁺ conjugates **11a-f**. Reagents and conditions: (a) TPP, 100 °C, 48 h; (b) (C₂H₅)₃N, ClCOOC₂H₅, DCM, r.t., 10 h; (c) BBr₃, anhydrous DCM, -78 °C to r.t., 12 h.; (d) BBr₃·S(CH₃)₂, anhydrous DCM, reflux, 2–3 h.

(7-((3,4,5-Trimethoxyphenyl)amino)7-oxoheptyl)triphenylphosphonium bromide (10b). Procedure A1. $\eta = 72\%$. ¹H NMR (CDCl₃): $\delta = 1.40 - 1.50$ (2H, m, CH₂(CH₂)₂P⁺), $1.54 - 1.65$ (2H, m, CH₂CH₂-P⁺), $1.67 - 1.76$ (2H, m, CH₂(CH₂)₃P⁺), $1.76 - 1.84$ (2H, m, CH₂-

CH₂)₄P⁺), 2.62 (2H, t, $J = 6.8$ Hz, CH₂(CH₂)₅P⁺), $3.57 - 3.69$ (2H, m, CH₂P⁺), 3.78 (3H, s, OCH₃), 3.79 (6H, s, $2 \times$ OCH₃), 7.46 (2H, H(2) and H(6)), $7.58 - 7.82$ (15H, m, PPh₃), 10.55 (1H, s, NH). ¹³C NMR (CDCl₃): $\delta = 22.0$ (d, $J_{CP} = 4.3$ Hz, CH₂(CH₂)₂P⁺), 22.2 (d, $J_{CP} = 50.1 -$

Hz, CH_2P^+), 24.7 ($\text{CH}_2(\text{CH}_2)_4\text{P}^+$), 26.5 ($\text{CH}_2(\text{CH}_2)_3\text{P}^+$), 28.4 (d, $J_{\text{CP}} = 16.7$ Hz, $\text{CH}_2\text{CH}_2\text{P}^+$), 36.1 ($\text{CH}_2(\text{CH}_2)_5\text{P}^+$), 56.2 ($2 \times \text{OCH}_3$), 61.0 (OCH_3), 97.6 (C(2) and C(6)), 118.4 (d, $J_{\text{CP}} = 85.9$ Hz, $3 \times \text{C}(1')$), 130.6 (d, $J_{\text{CP}} = 12.5$ Hz, $3 \times \text{C}(3')$ and $3 \times \text{C}(5')$), 133.6 (d, $J_{\text{CP}} = 10.0$ Hz, $3 \times \text{C}(2')$ and $3 \times \text{C}(6')$), 133.6 (C(4)), 135.2 (d, $J_{\text{CP}} = 3.0$ Hz, $3 \times \text{C}(4')$), 136.4 (C(1)), 152.9 (C(3) and C(5)), 173.2 (CO).

(9-((3,4-Dimethoxyphenyl)amino)-9-oxononyl)triphenylphosphonium bromide (10c). Procedure A1. $\eta = 80\%$. ^1H NMR (CDCl_3): $\delta = 1.23 - 1.41$ (6H, m, $(\text{CH}_2)_3(\text{CH}_2)_2\text{P}^+$), $1.54 - 1.75$ (6H, m, $(\text{CH}_2)_2(-\text{CH}_2)_3\text{CH}_2\text{CH}_2\text{P}^+$), 2.50 (2H, t, $J = 7.6$ Hz, $\text{CH}_2(\text{CH}_2)_7\text{P}^+$), 3.51 - 3.64 (2H, m, CH_2P^+), 3.79 (3H, s, OCH_3), 3.82 (3H, s, OCH_3), 6.68 (1H, d, $J = 8.7$ Hz, H(5)), 7.40 (1H, dd, $J = 2.4, 8.7$ Hz, H(6)), 7.61 - 7.85 (16H, m, PPh_3 and H(2)), 9.71 (1H, s, NH). ^{13}C NMR (CDCl_3): $\delta = 22.3$ (d, $J_{\text{CP}} = 4.5$ Hz, $\text{CH}_2(\text{CH}_2)_2\text{P}^+$), 22.6 (d, $J_{\text{CP}} = 50.1$ Hz, CH_2P^+), 25.3 ($\text{CH}_2(\text{CH}_2)_6\text{P}^+$), 27.7 ($(\text{CH}_2(\text{CH}_2)_5\text{P}^+$), 28.0 ($(\text{CH}_2)_2(-\text{CH}_2)_3\text{P}^+$), 29.8 (d, $J_{\text{CP}} = 15.6$ Hz, $\text{CH}_2\text{CH}_2\text{P}^+$), 37.4 ($\text{CH}_2(\text{CH}_2)_7\text{P}^+$), 56.0 (OCH_3), 56.2 (OCH_3), 105.0 (C(2)), 111.2 (C(6)), 111.8 (C(5)), 118.3 (d, $J_{\text{CP}} = 85.9$ Hz, $3 \times \text{C}(1')$), 130.6 (d, $J_{\text{CP}} = 12.5$ Hz, $3 \times \text{C}(3')$ and $3 \times \text{C}(5')$), 133.6 (d, $J_{\text{CP}} = 9.9$ Hz, $3 \times \text{C}(2')$ and $3 \times \text{C}(6')$), 133.6 (C(1)), 135.1 (d, $J_{\text{CP}} = 3.0$ Hz, $3 \times \text{C}(4')$), 144.7 (C(4)), 148.6 (C(3)), 172.7 (CO).

(9-((3,4,5-Trimethoxyphenyl)amino)-9-oxononyl)triphenylphosphonium bromide (10d). Procedure A1. $\eta = 69\%$. ^1H NMR (CDCl_3): $\delta = 1.27 - 1.41$ (6H, m, $(\text{CH}_2)_3(\text{CH}_2)_2\text{P}^+$), $1.56 - 1.76$ (6H, m, $(\text{CH}_2)_2(\text{CH}_2)_3\text{CH}_2\text{CH}_2\text{P}^+$), 2.53 (2H, t, $J = 7.6$ Hz, $\text{CH}_2(\text{CH}_2)_7\text{P}^+$), 3.50 - 3.62 (2H, m, CH_2P^+), 3.77 (3H, s, OCH_3), 3.79 (6H, s, $2 \times \text{OCH}_3$), 7.39 (2H, H(2) and H(6)), 7.65 - 7.83 (15H, m, PPh_3), 9.90 (1H, s, NH). ^{13}C NMR (CDCl_3): $\delta = 22.3$ (d, $J_{\text{CP}} = 4.3$ Hz, $\text{CH}_2(-\text{CH}_2)_2\text{P}^+$), 22.6 (d, $J_{\text{CP}} = 50.0$ Hz, CH_2P^+), 25.2 ($\text{CH}_2(\text{CH}_2)_6\text{P}^+$), 27.6 ($(\text{CH}_2(\text{CH}_2)_5\text{P}^+$), 27.9 ($(\text{CH}_2)_2(\text{CH}_2)_3\text{P}^+$), 29.7 (d, $J_{\text{CP}} = 15.4$ Hz, $\text{CH}_2\text{CH}_2\text{P}^+$), 37.5 ($\text{CH}_2(\text{CH}_2)_7\text{P}^+$), 56.1 ($2 \times \text{OCH}_3$), 60.9 (OCH_3), 97.6 (C(2) and C(6)), 118.3 (d, $J_{\text{CP}} = 85.9$ Hz, $3 \times \text{C}(1')$), 130.6 (d, $J_{\text{CP}} = 12.5$ Hz, $3 \times \text{C}(3')$ and $3 \times \text{C}(5')$), 133.6 (d, $J_{\text{CP}} = 9.9$ Hz, $3 \times \text{C}(2')$ and $3 \times \text{C}(6')$), 135.2 (d, $J_{\text{CP}} = 3.0$ Hz, $3 \times \text{C}(4')$), 133.6 (C(4)), 136.1 (C(1)), 152.8 (C(3) and C(5)), 173.2 (CO).

(11-((3,4-Dimethoxyphenyl)amino)-11-oxoundecyl)triphenylphosphonium bromide (10e). Procedure A1. $\eta = 85\%$. ^1H NMR (CDCl_3): $\delta = 1.05 - 1.27$ (10H, m, $(\text{CH}_2)_5(\text{CH}_2)_2\text{P}^+$), $1.41 - 1.63$ (6H, m, $(\text{CH}_2)_2(\text{CH}_2)_5\text{CH}_2\text{CH}_2\text{P}^+$), 2.43 (2H, t, $J = 7.4$ Hz, $\text{CH}_2(\text{CH}_2)_9\text{P}^+$), 3.36 - 3.47 (2H, m, CH_2P^+), 3.69 (3H, s, OCH_3), 3.71 (3H, s, OCH_3), 6.56 (1H, d, $J = 8.7$ Hz, H(5)), 7.27 (1H, dd, $J = 2.6, 8.9$ Hz, H(6)), 7.58 - 7.78 (15H, m, PPh_3 and H(2)), 10.01 (1H, s, NH). ^{13}C NMR (CDCl_3): $\delta = 22.4$ (d, $J_{\text{CP}} = 4.4$ Hz, $\text{CH}_2(\text{CH}_2)_2\text{P}^+$), 22.5 (d, $J_{\text{CP}} = 50.3$ Hz, CH_2P^+), 25.6 ($\text{CH}_2(\text{CH}_2)_8\text{P}^+$), 28.5 ($\text{CH}_2(\text{CH}_2)_7\text{P}^+$), 28.7 ($\text{CH}_2(-\text{CH}_2)_6\text{P}^+$), 28.8 ($\text{CH}_2\text{CH}_2\text{CH}_2(\text{CH}_2)_3\text{P}^+$), 28.9 ($\text{CH}_2(\text{CH}_2)_4\text{P}^+$), 30.2 (d, $J_{\text{CP}} = 15.5$ Hz, $\text{CH}_2\text{CH}_2\text{P}^+$), 37.0 ($\text{CH}_2(\text{CH}_2)_9\text{P}^+$), 55.8 (OCH_3), 56.1 (OCH_3), 105.0 (C(2)), 111.2 (C(6)), 111.9 (C(5)), 118.1 (d, $J_{\text{CP}} = 85.9$ Hz, $3 \times \text{C}(1')$), 130.6 (d, $J_{\text{CP}} = 12.5$ Hz, $3 \times \text{C}(3')$ and $3 \times \text{C}(5')$), 133.4 (d, $J_{\text{CP}} = 9.9$ Hz, $3 \times \text{C}(2')$ and $3 \times \text{C}(6')$), 133.7 (C(1)), 135.2 (d, $J_{\text{CP}} = 2.9$ Hz, $3 \times \text{C}(4')$), 144.6 (C(4)), 148.5 (C(3)), 172.7 (CO).

(11-((3,4,5-Trimethoxyphenyl)amino)-11-oxoundecyl)triphenylphosphonium bromide (10f). Procedure A1. $\eta = 65\%$. ^1H NMR (CDCl_3): $\delta = 1.15 - 1.38$ (10H, m, $(\text{CH}_2)_5(\text{CH}_2)_2\text{P}^+$), $1.47 - 1.77$ (6H, m, $(\text{CH}_2)_2(\text{CH}_2)_5\text{CH}_2\text{CH}_2\text{P}^+$), 2.53 (2H, t, $J = 7.4$ Hz, $\text{CH}_2(\text{CH}_2)_9\text{P}^+$), 3.49 - 3.60 (2H, m, CH_2P^+), 3.75 (9H, s, OCH_3), 7.29 (2H, H(2) and H(6)), 7.63 - 7.82 (15H, m, PPh_3), 10.00 (1H, s, NH). ^{13}C NMR (CDCl_3): $\delta = 22.6$ (d, $J_{\text{CP}} = 4.6$ Hz, $\text{CH}_2(\text{CH}_2)_2\text{P}^+$), 22.6 (d, $J_{\text{CP}} = 50.0$ Hz,

CH_2P^+), 25.4 ($\text{CH}_2(\text{CH}_2)_8\text{P}^+$), 28.4 ($\text{CH}_2(\text{CH}_2)_7\text{P}^+$), 28.5 ($\text{CH}_2(\text{CH}_2)_6\text{P}^+$), 28.7 ($\text{CH}_2\text{CH}_2\text{CH}_2(\text{CH}_2)_3\text{P}^+$), 28.8 ($\text{CH}_2(\text{CH}_2)_4\text{P}^+$), 30.2 (d, $J_{\text{CP}} = 15.6$ Hz, $\text{CH}_2\text{CH}_2\text{P}^+$), 37.2 ($\text{CH}_2(\text{CH}_2)_9\text{P}^+$), 56.2 ($2 \times \text{OCH}_3$), 61.0 (OCH_3), 97.8 (C(2) and C(6)), 118.4 (d, $J_{\text{CP}} = 85.9$ Hz, $3 \times \text{C}(1')$), 130.7 (d, $J_{\text{CP}} = 12.5$ Hz, $3 \times \text{C}(3')$ and $3 \times \text{C}(5')$), 133.6 (d, $J_{\text{CP}} = 10.0$ Hz, $3 \times \text{C}(2')$ and $3 \times \text{C}(6')$), 133.6 (C(4)), 135.3 (d, $J_{\text{CP}} = 3.0$ Hz, $3 \times \text{C}(4')$), 136.2 (C(1)), 152.9 (C(3) and C(5)), 173.2 (CO).

General procedure for the synthesis of bromo (3a-f) and methanesulfonate derivatives (3g-n)

Bromo (**3a-f**) and methanesulfonate derivatives (**3g-n**) were obtained following the procedures **B1** and **B2**, respectively.

Procedure B1. Compounds **2a-f** (1 mmol) and 1,2-dibromotetrachloroethane (1 mmol) were dissolved in tetrahydrofuran (20 mL). Then, 1,2-bis(diphenylphosphine)ethane (diphos, 0.5 mmol) was added, and the reaction mixture was stirred at room temperature for 20 h. Upon completion, the reaction mixture was filtered through Celite and concentrated under reduced pressure. The oil residue obtained was purified by flash column chromatography (silica gel). The reaction conditions and work-up were previously described in literature [19,20].

Procedure B2. Compounds **2g-n** (1 mmol) were dissolved in dichloromethane (10 mL) and triethylamine (1.5 mmol). The mixture was stirred at room temperature for 10 min. Then, a solution of methanesulfonyl chloride (1.5 mmol) in tetrahydrofuran (5 mL) was added dropwise over 20 min, and the reaction mixture stirred at room temperature for 12 h. Upon completion, the mixture was extracted, and the combined organic layers were dried over Na_2SO_4 , filtered and concentrated. The reaction conditions and work-up were previously described in literature [21].

The spectroscopic data of compounds **3a-n** were previously described in literature [19–21].

General procedure for the synthesis of triphenylphosphonium salts (4a-t, 7 and 9a-c)

Triphenylphosphonium salts **4a-t**, **7** and **9a-c** were obtained by two different synthetic strategies: procedure **C1** (compounds **4a-t** and **9a-c**) and procedure **C2** (compound **7**).

Procedure C1. Bromo or methanesulfonate derivatives (**3a-t** or **8a-c**, 1 mmol) were heated with triphenylphosphine (TPP, 1 mmol) at 100–130 °C for 48 h under argon atmosphere. The resulting products were purified by flash column chromatography. The reaction conditions and work-up were previously described in literature [18–21].

Procedure C2. A mixture containing the appropriate *N*-(bromoalkyl)phthalimide (1 mmol) and triphenylphosphine (1.2 mmol) was thoroughly mixed under argon atmosphere and heated at 130 °C for 2 h, protected from the light. Then, ethanol and butylamine (10 mmol) were added, and the mixture was refluxed for 2 h. Upon completion, the solvent was partially concentrated, and water was added. The solid obtained was filtered off under reduced pressure and the filtrate was extracted with dichloromethane. The aqueous phase was concentrated. The crude product was used without further purification in the next step.

The spectroscopic data of compounds **4a-t** were previously described [18–21].

(8-Aminoocetyl)triphenylphosphonium bromide (7). Procedure C2. $\eta = 87\%$. ^1H NMR (MeOD): $\delta = 1.23 - 1.44$ (6H, m, $(\text{CH}_2)_3(-\text{CH}_2)_2\text{P}^+$), $1.47 - 1.61$ (4H, m, $(\text{CH}_2)_2\text{CH}_2\text{P}^+$), $1.62 - 1.73$ (2H, m, $\text{CH}_2(\text{CH}_2)_6\text{P}^+$), 2.74 (2H, t, $J = 7.5$ Hz, $\text{CH}_2(\text{CH}_2)_7\text{P}^+$), 3.37 - 3.46 (2H, m, CH_2P^+), 7.73 - 7.94 (15H, m, PPh_3). ^{13}C NMR (MeOD):

$\delta = 22.7$ (d, $J_{CP} = 51.0$ Hz, CH_2P^+), 23.5 (d, $J_{CP} = 4.4$ Hz, $\text{CH}_2(\text{CH}_2)_2\text{P}^+$), 27.5 ($\text{CH}_2(\text{CH}_2)_5\text{P}^+$), 29.7 ($\text{CH}_2(\text{CH}_2)_3\text{P}^+$), 30.0 ($\text{CH}_2(\text{CH}_2)_4\text{P}^+$), 31.2 ($\text{CH}_2(\text{CH}_2)_6\text{P}^+$), 31.5 (d, $J_{CP} = 16.2$ Hz, $\text{CH}_2\text{CH}_2\text{P}^+$), 41.6 ($\text{CH}_2(\text{CH}_2)_7\text{P}^+$), 120.0 (d, $J_{CP} = 86.4$ Hz, $3 \times \text{C}(1')$), 131.5 (d, $J_{CP} = 12.5$ Hz, $3 \times \text{C}(3')$ and $3 \times \text{C}(5')$), 134.8 (d, $J_{CP} = 10.1$ Hz, $3 \times \text{C}(2')$ and $3 \times \text{C}(6')$), 136.3 (d, $J_{CP} = 3.1$ Hz, $3 \times \text{C}(4')$).

(6-Carboxyhexyl)triphenylphosphonium bromide (9a). Procedure C1. $\eta = 92\%$. $^1\text{H NMR}$ (CDCl_3): $\delta = 1.23 - 1.32$ (2H, m, $\text{CH}_2(-\text{CH}_2)_2\text{P}^+$), 1.40 - 1.49 (2H, m, $\text{CH}_2\text{CH}_2\text{P}^+$), 1.52 - 1.62 (4H, m, $(\text{CH}_2)_2(\text{CH}_2)_3\text{P}^+$), 2.27 (2H, t, $J = 7.2$ Hz, $\text{CH}_2(\text{CH}_2)_5\text{P}^+$), 3.45 - 3.55 (2H, m, CH_2P^+), 7.62 - 7.79 (15H, m, PPh_3). $^{13}\text{C NMR}$ (CDCl_3): $\delta = 22.1$ (d, $J_{CP} = 4.5$ Hz, $\text{CH}_2(\text{CH}_2)_2\text{P}^+$), 22.4 (d, $J_{CP} = 50.4$ Hz, CH_2P^+), 24.2 ($\text{CH}_2(\text{CH}_2)_4\text{P}^+$), 27.9 ($\text{CH}_2(\text{CH}_2)_3\text{P}^+$), 29.5 (d, $J_{CP} = 16.1$ - Hz, $\text{CH}_2\text{CH}_2\text{P}^+$), 34.3 ($\text{CH}_2(\text{CH}_2)_5\text{P}^+$), 118.1 (d, $J_{CP} = 85.9$ Hz, $3 \times \text{C}(1')$), 130.6 (d, $J_{CP} = 12.5$ Hz, $3 \times \text{C}(3')$ and $3 \times \text{C}(5')$), 133.6 (d, $J_{CP} = 10.0$ Hz, $3 \times \text{C}(2')$ and $3 \times \text{C}(6')$), 135.2 (d, $J_{CP} = 2.9$ Hz, $3 \times \text{C}(4')$), 176.3 (CO).

(8-Carboxyoctyl)triphenylphosphonium bromide (9b). Procedure C1. $\eta = 98\%$. $^1\text{H NMR}$ (CDCl_3): $\delta = 1.18 - 1.34$ (6H, m, $(\text{CH}_2)_3(-\text{CH}_2)_2\text{P}^+$), 1.51 - 1.66 (6H, m, $(\text{CH}_2)_2(\text{CH}_2)_3\text{CH}_2\text{CH}_2\text{P}^+$), 2.35 (2H, t, $J = 7.3$ Hz, $\text{CH}_2(\text{CH}_2)_7\text{P}^+$), 3.60 - 3.72 (2H, m, CH_2P^+), 7.67 - 7.86 (15H, m, PPh_3). $^{13}\text{C NMR}$ (CDCl_3): $\delta = 22.6$ (d, $J_{CP} = 4.8$ Hz, $\text{CH}_2(-\text{CH}_2)_2\text{P}^+$), 22.8 (d, $J_{CP} = 49.6$ Hz, CH_2P^+), 24.6 ($\text{CH}_2(\text{CH}_2)_6\text{P}^+$), 28.3 ($(\text{CH}_2(\text{CH}_2)_5\text{P}^+)$), 28.4 ($(\text{CH}_2)_2(\text{CH}_2)_3\text{P}^+$), 30.1 (d, $J_{CP} = 15.8$ Hz, $\text{CH}_2\text{CH}_2\text{P}^+$), 34.6 ($\text{CH}_2(\text{CH}_2)_7\text{P}^+$), 118.5 (d, $J_{CP} = 85.8$ Hz, $3 \times \text{C}(1')$), 130.7 (d, $J_{CP} = 12.6$ Hz, $3 \times \text{C}(3')$ and $3 \times \text{C}(5')$), 133.8 (d, $J_{CP} = 9.9$ - Hz, $3 \times \text{C}(2')$ and $3 \times \text{C}(6')$), 135.2 (d, $J_{CP} = 3.1$ Hz, $3 \times \text{C}(4')$), 176.8 (CO).

(10-Carboxydecyl)triphenylphosphonium bromide (9c). Procedure C1. $\eta = 98\%$. $^1\text{H NMR}$ (CDCl_3): $\delta = 1.12 - 1.30$ (10H, m, $(\text{CH}_2)_5(\text{CH}_2)_2\text{P}^+$), 1.50 - 1.65 (6H, m, $(\text{CH}_2)_2(\text{CH}_2)_5\text{CH}_2\text{CH}_2\text{P}^+$), 2.34 (2H, t, $J = 7.4$ Hz, $\text{CH}_2(\text{CH}_2)_9\text{P}^+$), 3.58 - 3.68 (2H, m, CH_2P^+), 7.65 - 7.85 (15H, m, PPh_3). $^{13}\text{C NMR}$ (CDCl_3): $\delta = 22.7$ (d, $J_{CP} = 4.6$ Hz, $\text{CH}_2(\text{CH}_2)_2\text{P}^+$), 22.8 (d, $J_{CP} = 50.1$ Hz, CH_2P^+), 24.8 ($\text{CH}_2(\text{CH}_2)_8\text{P}^+$), 28.8 ($(\text{CH}_2)_2(\text{CH}_2)_2\text{CH}_2(\text{CH}_2)_3\text{P}^+$), 28.9 ($\text{CH}_2(\text{CH}_2)_5\text{P}^+$), 29.0 ($\text{CH}_2(-\text{CH}_2)_4\text{P}^+$), 30.4 (d, $J_{CP} = 15.6$ Hz, $\text{CH}_2\text{CH}_2\text{P}^+$), 34.4 ($\text{CH}_2(\text{CH}_2)_9\text{P}^+$), 118.4 (d, $J_{CP} = 85.8$ Hz, $3 \times \text{C}(1')$), 130.7 (d, $J_{CP} = 12.5$ Hz, $3 \times \text{C}(3')$ and $3 \times \text{C}(5')$), 133.7 (d, $J_{CP} = 10.0$ Hz, $3 \times \text{C}(2')$ and $3 \times \text{C}(6')$), 135.2 (d, $J_{CP} = 2.9$ Hz, $3 \times \text{C}(4')$), 177.3 (CO).

General procedure to obtain lipophilic TPP^+ conjugates 5a-x and 11a-f

The TPP^+ conjugates **5a-x** and **11a-f** were synthesized following two different procedures: method **D1** for compounds **5a-x**, **11b**, **11d** and **11f** and method **D2** for compounds **11a**, **11c** and **11e**.

Procedure D1. A solution of compounds **4a-x**, **10b**, **10d** or **10f** (1 mmol) in anhydrous dichloromethane (15 mL) was stirred under argon atmosphere and cooled at a temperature below -70°C . Then, boron tribromide 1 M (5-7 mmol) was added. The reaction mixture was stirred at -70°C for 10 min and then allowed to reach room temperature for additional 12 h. Upon completion, the reaction mixture was cautiously quenched with water (40 mL). After removing the water, the product was dissolved in methanol, dried over anhydrous sodium sulphate, filtered and concentrated. The residue was purified by flash column chromatography (silica gel, dichloromethane:methanol (9:1) to (8:2)). The reaction conditions and work-up were previously described in literature [18-21].

Procedure D2. To a solution of compounds **10a**, **10c** or **10e** (1 mmol) in dichloromethane (10 mL), boron tribromide dimethyl

sulphide complex (6.0 mmol) was added. The reaction mixture was refluxed for 2-3 h. Upon completion, the reaction mixture was cautiously quenched with water (40 mL). After removing the water, the product was dissolved in methanol, dried over anhydrous sodium sulphate, filtered and concentrated. The residue was purified by flash column chromatography (silica gel, dichloromethane:methanol (9:1) to (8:2)). The reaction was followed by TLC (silica gel, mobile phase with dichloromethane:methanol (9:1)). The reaction conditions and work-up were previously described in literature [18-21].

The spectroscopic data of compounds **5a-t** were previously described in literature [18-21].

(8-(2-(3,4-dihydroxyphenyl)acetamido)octyl)triphenylphosphonium bromide (5u). Procedure D1. $\eta = 50\%$. $^1\text{H NMR}$ (MeOD): $\delta = 1.17 - 1.33$ (6H, m, $(\text{CH}_2)_3\text{CH}_2\text{CH}_2\text{CH}_2\text{P}^+$), 1.38 - 1.55 (4H, m, $\text{CH}_2\text{CH}_2\text{CH}_2\text{P}^+$), 1.59 - 1.69 (2H, m, $\text{CH}_2(\text{CH}_2)_6\text{P}^+$), 3.12 (2H, t, $J = 7.0$ Hz, $\text{CH}_2(\text{CH}_2)_7\text{P}^+$), 3.28 - 3.42 (4H, m, $(\text{CH}_2\text{P}^+$ and $\text{CH}_2\text{CONH})$), 6.58 (1H, dd, $J = 8.1, 2.1$ Hz, H(6)), 6.68 (1H, d, $J = 8.1$ Hz, H(5)), 6.72 (1H, d, $J = 2.1$ Hz), 7.71 - 7.95 (15H, m, PPh_3). $^{13}\text{C NMR}$ (MeOD): $\delta = 22.6$ (d, $J_{CP} = 51.3$ Hz, CH_2P^+), 23.4 (d, $J_{CP} = 4.4$ Hz, $\text{CH}_2(\text{CH}_2)_2\text{P}^+$), 27.5 ($\text{CH}_2(\text{CH}_2)_5\text{P}^+$), 29.6 ($\text{CH}_2(\text{CH}_2)_3\text{P}^+$), 29.8 ($\text{CH}_2(\text{CH}_2)_4\text{P}^+$), 30.2 ($\text{CH}_2(\text{CH}_2)_6\text{P}^+$), 31.3 (d, $J_{CP} = 16.1$ Hz, $\text{CH}_2\text{CH}_2\text{P}^+$), 40.3 ($\text{CH}_2(\text{CH}_2)_7\text{P}^+$), 43.5 (CH_2CONH), 116.4 (C(2)), 117.2 (C(5)), 120.0 (d, $J_{CP} = 86.1$ - Hz, $3 \times \text{C}(1')$), 121.5 (C(6)), 128.5 (C(1)), 131.5 (d, $J_{CP} = 12.5$ Hz, $3 \times \text{C}(3')$ and $3 \times \text{C}(5')$), 134.8 (d, $J_{CP} = 9.7$ Hz, $3 \times \text{C}(6')$ and $3 \times \text{C}(2')$), 136.3 (d, $J_{CP} = 2.9$ Hz, $3 \times \text{C}(4')$), 145.4 (C(4)), 146.4 (C(3)), 174.7 (CO).

(8-(2-(3,4,5-trihydroxyphenyl)acetamido)octyl)triphenylphosphonium bromide (5v). Procedure D1. $\eta = 20\%$. $^1\text{H NMR}$ (MeOD): $\delta = 1.2 - 1.3$ (6H, m, $(\text{CH}_2)_3\text{CH}_2\text{CH}_2\text{CH}_2\text{P}^+$), 1.4 - 1.5 (4H, m, $\text{CH}_2\text{CH}_2\text{CH}_2\text{P}^+$), 1.6 - 1.7 (2H, m, $\text{CH}_2(\text{CH}_2)_6\text{P}^+$), 3.1 (2H, t, $J = 6.9$ Hz, $\text{CH}_2(-\text{CH}_2)_7\text{P}^+$), 3.2 (2H, s, CH_2CONH), 3.3 - 3.4 (2H, m, CH_2P^+), 6.3 (2H, s, H(2) and H(6)), 7.7 - 7.9 (15H, m, PPh_3). $^{13}\text{C NMR}$ (MeOD): $\delta = 22.6$ (d, $J_{CP} = 51.0$ Hz, CH_2P^+), 23.5 (d, $J_{CP} = 4.4$ Hz, $\text{CH}_2(\text{CH}_2)_2\text{P}^+$), 27.4 ($\text{CH}_2(\text{CH}_2)_5\text{P}^+$), 29.6 ($\text{CH}_2(\text{CH}_2)_3\text{P}^+$), 29.8 ($\text{CH}_2(\text{CH}_2)_4\text{P}^+$), 30.2 ($\text{CH}_2(\text{CH}_2)_6\text{P}^+$), 31.3 (d, $J_{CP} = 16.1$ Hz, $\text{CH}_2\text{CH}_2\text{P}^+$), 40.3 ($\text{CH}_2(\text{CH}_2)_7\text{P}^+$), 43.7 (CH_2CONH), 109.1 (C(2) and $3 \times \text{C}(6)$), 120.0 (d, $J_{CP} = 86.2$ - Hz, $3 \times \text{C}(1')$), 127.8 (C(1)), 131.5 (d, $J_{CP} = 12.7$ Hz, $3 \times \text{C}(3')$ and $3 \times \text{C}(5')$), 133.2 (C(4)), 134.8 (d, $J_{CD} = 9.9$ Hz, $3 \times \text{C}(6')$ and $3 \times \text{C}(2')$), 136.2 (d, $J_{CD} = 3.1$ Hz, $3 \times \text{C}(4')$), 147.1 (C(5) and C(3)), 174.6 (CO).

(8-(3-(3,4-dihydroxyphenyl)propanamido)octyl)triphenylphosphonium bromide (5w). Procedure D1. $\eta = 62\%$. $^1\text{H NMR}$ (MeOD): $\delta = 1.12 - 1.42$ (8H, m, $(\text{CH}_2)_4\text{CH}_2\text{CH}_2\text{P}^+$), 1.48 - 1.58 (2H, m, $\text{CH}_2\text{CH}_2\text{P}^+$), 1.61 - 1.74 (2H, m, $\text{CH}_2(\text{CH}_2)_6\text{P}^+$), 2.38 (2H, t, $J = 7.5$ Hz, CH_2CONH), 2.73 (2H, t, $J = 7.5$ Hz, $\text{CH}_2\text{CH}_2\text{CONH}$), 3.08 (2H, t, $J = 6.9$ Hz, $\text{CH}_2(\text{CH}_2)_7\text{P}^+$), 3.34 - 3.45 (2H, m, CH_2P^+), 6.49 (1H, dd, $J = 8.0, 2.1$ Hz, H(6)), 6.61 (1H, d, $J = 2.1$ Hz, H(2)), 6.63 (1H, d, $J = 8.0$ Hz, H(5)), 7.70 - 7.93 (15H, m, PPh_3). $^{13}\text{C NMR}$ (MeOD): $\delta = 22.7$ (d, $J_{CP} = 50.8$ Hz, CH_2P^+), 23.5 (d, $J_{CP} = 4.4$ Hz, $\text{CH}_2(\text{CH}_2)_2\text{P}^+$), 27.6 ($\text{CH}_2(\text{CH}_2)_5\text{P}^+$), 29.7 ($\text{CH}_2(\text{CH}_2)_3\text{P}^+$), 30.0 ($\text{CH}_2(\text{CH}_2)_4\text{P}^+$), 30.3 ($\text{CH}_2(\text{CH}_2)_6\text{P}^+$), 31.5 (d, $J_{CP} = 16.1$ Hz, $\text{CH}_2\text{CH}_2\text{P}^+$), 32.5 ($\text{CH}_2\text{CH}_2\text{CONH}$), 39.4 ($\text{CH}_2\text{CH}_2\text{CONH}$), 40.2 ($\text{CH}_2(\text{CH}_2)_7\text{P}^+$), 116.3 (C(5)), 116.7 (C(2)), 120.1 (d, $J_{CP} = 86.3$ Hz, $3 \times \text{C}(1')$), 120.6 (C(6)), 131.6 (d, $J_{CP} = 12.6$ Hz, $3 \times \text{C}(3')$ and $3 \times \text{C}(5')$), 133.7 (C(1)), 134.9 (d, $J_{CP} = 9.9$ Hz, $3 \times \text{C}(6')$ and $3 \times \text{C}(2')$), 136.3 (d, $J = 3.1$ Hz, $3 \times \text{C}(4')$), 144.7 (C(3)), 146.2 (C(4)), 175.4 (CO).

(8-(3-(3,4,5-trihydroxyphenyl)propanamido)octyl)triphenylphosphonium bromide (5x). Procedure D1. $\eta = 61\%$. $^1\text{H NMR}$ (MeOD): $\delta = 1.10 - 1.43$ (8H, m, $(\text{CH}_2)_4\text{CH}_2\text{CH}_2\text{P}^+$), 1.49 - 1.59

(2H, *m*, CH₂CH₂P⁺), 1.58 – 1.73 (2H, *m*, CH₂(CH₂)₆P⁺), 2.37 (2H, *t*, *J* = 7.5 Hz, CH₂CONH), 2.67 (2H, *t*, *J* = 7.5 Hz, CH₂CH₂CONH), 3.08 (2H, *t*, *J* = 6.9 Hz, CH₂(CH₂)₇P⁺), 3.34 – 3.46 (2H, *m*, CH₂P⁺), 6.19 (2H, *s*, C(6) and C(2)), 7.69 – 7.98 (15H, *m*, PPh₃). ¹³C NMR (MeOD): δ = 22.7 (*d*, *J*_{CP} = 51.0 Hz, CH₂P⁺), 23.5 (*d*, *J*_{CP} = 4.3 Hz, CH₂(CH₂)₂P⁺), 27.6 (CH₂(CH₂)₅P⁺), 29.6 (CH₂(CH₂)₃P⁺), 29.9 (CH₂(CH₂)₄P⁺), 30.2 (CH₂(CH₂)₆P⁺), 31.4 (*d*, *J*_{CP} = 16.0 Hz, CH₂CH₂P⁺), 32.7 (CH₂CH₂CONH), 39.3 (CH₂CH₂CONH), 40.2 (CH₂(CH₂)₇P⁺), 108.3 (C(6) and C(2)), 120.0 (*d*, *J*_{CP} = 86.4 Hz, 3 × C(1')), 131.5 (*d*, *J*_{CP} = 12.5 Hz, 3 × C(3') and 3 × C(5')), 132.5 (C(1)), 133.1 (C(4)), 134.8 (*d*, *J*_{CP} = 10.0 Hz, 3 × C(6') and 3 × C(2')), 136.2 (*d*, *J*_{CP} = 3.1 Hz, 3 × C(4')), 146.9 (C(5) and C(3)), 175.3 (CO).

(7-((3,4-dihydroxyphenyl)amino)-7-oxoheptyl)triphenylphosphonium bromide (11a). Procedure D2. η = 36 %. ¹H NMR (DMSO *d*₆): δ = 1.24 – 1.34 (2H, *m*, CH₂(CH₂)₂P⁺), 1.44 – 1.57 (6H, *m*, (CH₂)₂CH₂CH₂CH₂P⁺), 2.20 (2H, *t*, *J* = 7.2 Hz, CH₂(CH₂)₅P⁺), 3.52 – 3.62 (2H, *m*, CH₂P⁺), 6.60 (1H, *d*, *J* = 8.5 Hz, H(5)), 6.77 (1H, *dd*, *J* = 2.4, 8.5 Hz, H(6)), 7.12 (1H, *d*, *J* = 2.4 Hz, H(2)), 7.73 – 7.93 (15H, *m*, PPh₃), 8.71 (2H, *s*, 2 × OH), 9.50 (1H, *s*, NH). ¹³C NMR (DMSO *d*₆): δ = 20.2 (*d*, *J*_{CP} = 49.7 Hz, CH₂P⁺), 21.6 (*d*, *J*_{CP} = 4.0 Hz, CH₂(CH₂)₂P⁺), 24.8 (CH₂(CH₂)₄P⁺), 27.8 (CH₂(CH₂)₃P⁺), 29.6 (*d*, *J*_{CP} = 16.8 Hz, CH₂CH₂P⁺), 36.1 (CH₂(CH₂)₅P⁺), 107.9 (C(2)), 110.2 (C(6)), 115.1 (C(5)), 118.6 (*d*, *J*_{CP} = 85.7 Hz, 3 × C(1')), 130.2 (*d*, *J*_{CP} = 12.4 Hz, 3 × C(3') and 3 × C(5')), 131.5 (C(1)), 133.6 (*d*, *J*_{CP} = 10.1 Hz, 3 × C(2') and 3 × C(6')), 134.9 (*d*, *J*_{CP} = 2.8 Hz, 3 × C(4')), 141.0 (C(4)), 144.8 (C(3)), 170.2 (CO).

(7-((3,4,5-trihydroxyphenyl)amino)7-oxoheptyl)triphenylphosphonium bromide (11b). Procedure D1. η = 55 %. ¹H NMR (DMSO *d*₆): δ = 1.21 – 1.34 (2H, *m*, CH₂(CH₂)₂P⁺), 1.40 – 1.57 (6H, *m*, (CH₂)₂CH₂CH₂CH₂P⁺), 2.18 (2H, *t*, *J* = 7.3 Hz, CH₂(CH₂)₅P⁺), 3.51 – 3.62 (2H, *m*, CH₂P⁺), 6.60 (2H, *m*, H(2) and H(6)), 7.71 – 7.93 (15H, *m*, PPh₃), 9.37 (1H, *s*, NH). ¹³C NMR (DMSO *d*₆): δ = 20.2 (*d*, *J*_{CP} = 49.5 Hz, CH₂P⁺), 21.7 (*d*, *J*_{CP} = 4.5 Hz, CH₂(CH₂)₂P⁺), 24.9 (CH₂(-CH₂)₄P⁺), 27.8 (CH₂(CH₂)₃P⁺), 29.7 (*d*, *J*_{CP} = 16.4 Hz, CH₂CH₂P⁺), 36.2 (CH₂(CH₂)₅P⁺), 98.9 (C(2) and C(6)), 118.6 (*d*, *J*_{CP} = 85.6 Hz, 3 × C(1')), 128.8 (C(4)), 130.2 (*d*, *J*_{CP} = 12.4 Hz, 3 × C(3') and 3 × C(5')), 130.9 (C(1)), 133.6 (*d*, *J*_{CP} = 10.1 Hz, 3 × C(2') and 3 × C(6')), 134.9 (*d*, *J*_{CP} = 3.2 Hz, 3 × C(4')), 145.8 (C(3) and C(5)), 170.2 (CO).

(9-((3,4-dihydroxyphenyl)amino)-9-oxononyl)triphenylphosphonium bromide (11c). Procedure D2. η = 62 %. ¹H NMR (DMSO *d*₆): δ = 1.15 – 1.33 (6H, *m*, (CH₂)₃(CH₂)₂P⁺), 1.36 – 1.64 (6H, *m*, (CH₂)₂(CH₂)₃CH₂CH₂P⁺), 2.20 (2H, *t*, *J* = 7.4 Hz, CH₂(CH₂)₇P⁺), 3.48 – 3.65 (2H, *m*, CH₂P⁺), 6.60 (1H, *d*, *J* = 8.5 Hz, H(5)), 6.77 (1H, *dd*, *J* = 2.5, 8.5 Hz, H(6)), 7.13 (1H, *d*, *J* = 2.4 Hz, H(2)), 7.63 – 8.00 (15H, *m*, PPh₃), 9.49 (1H, *s*, NH). ¹³C NMR (DMSO *d*₆): δ = 20.1 (*d*, *J*_{CP} = 49.9 Hz, CH₂P⁺), 21.7 (*d*, *J*_{CP} = 4.4 Hz, CH₂(CH₂)₂P⁺), 25.2 (CH₂(CH₂)₆P⁺), 28.0 ((CH₂(CH₂)₅P⁺), 28.5 ((CH₂)₂(CH₂)₃P⁺), 29.8 (*d*, *J*_{CP} = 16.7 Hz, CH₂CH₂P⁺), 36.3 (CH₂(CH₂)₇P⁺), 107.9 (C(2)), 110.3 (C(6)), 115.2 (C(5)), 118.6 (*d*, *J*_{CP} = 85.6 Hz, 3 × C(1')), 130.2 (*d*, *J*_{CP} = 12.4 Hz, 3 × C(3') and 3 × C(5')), 131.5 (*d*, *J*_{CP} = 10.1 Hz, 3 × C(2') and 3 × C(6')), 134.9 (*d*, *J*_{CP} = 2.9 Hz, 3 × C(4')), 134.9 (C(1)), 141.0 (C(4)), 144.8 (C(3)), 170.4 (CO).

(9-((3,4,5-trihydroxyphenyl)amino)9-oxononyl)triphenylphosphonium bromide (11d). Procedure D1. η = 90 %. ¹H NMR (DMSO *d*₆): δ = 1.13 – 1.32 (6H, *m*, (CH₂)₃(CH₂)₂P⁺), 1.38 – 1.59 (6H, *m*, (CH₂)₂(CH₂)₃CH₂CH₂P⁺), 2.19 (2H, *t*, *J* = 7.3 Hz, CH₂(CH₂)₇P⁺), 3.51 – 3.64 (2H, *m*, CH₂P⁺), 6.61 (2H, H(2) and H(6)), 7.70 – 7.95 (15H, *m*, PPh₃), 9.37 (1H, *s*, NH). ¹³C NMR (DMSO *d*₆):

δ = 20.1 (*d*, *J*_{CP} = 50.0 Hz, CH₂P⁺), 21.7 (*d*, *J*_{CP} = 4.5 Hz, CH₂(CH₂)₂P⁺), 25.2 (CH₂(CH₂)₆P⁺), 28.0 ((CH₂(CH₂)₅P⁺), 28.5 ((CH₂)₂(CH₂)₃P⁺), 29.8 (*d*, *J*_{CP} = 16.2 Hz, CH₂CH₂P⁺), 36.3 (CH₂(CH₂)₇P⁺), 99.0 (C(2) and C(6)), 118.6 (*d*, *J*_{CP} = 85.6 Hz, 3 × C(1')), 128.8 (C(4)), 130.2 (*d*, *J*_{CP} = 12.4 Hz, 3 × C(3') and 3 × C(5')), 130.9 (C(1)), 133.6 (*d*, *J*_{CP} = 10.1 Hz, 3 × C(2') and 3 × C(6')), 134.9 (*d*, *J*_{CP} = 2.9 Hz, 3 × C(4')), 145.7 (C(3) and C(5)), 170.4 (CO).

(11-((3,4-dihydroxyphenyl)amino)-11-oxoundecyl)triphenylphosphonium bromide (11e). Procedure D2. η = 41 %. ¹H NMR (DMSO *d*₆): δ = 1.10 – 1.33 (10H, *m*, (CH₂)₅(CH₂)₂P⁺), 1.36 – 1.63 (6H, *m*, (CH₂)₂(CH₂)₅CH₂CH₂P⁺), 2.21 (2H, *t*, *J* = 7.4 Hz, CH₂(CH₂)₉P⁺), 3.48 – 3.62 (2H, *m*, CH₂P⁺), 6.60 (1H, *d*, *J* = 8.5 Hz, H(5)), 6.77 (1H, *dd*, *J* = 2.4, 8.5 Hz, H(6)), 7.13 (1H, *d*, *J* = 2.4 Hz, H(2)), 7.67 – 7.98 (15H, *m*, PPh₃), 8.54 (1H, *s*, OH), 8.85 (1H, *s*, OH), 9.49 (1H, *s*, NH). ¹³C NMR (DMSO *d*₆): δ = 20.1 (*d*, *J*_{CP} = 49.9 Hz, CH₂P⁺), 21.7 (*d*, *J*_{CP} = 4.4 Hz, CH₂(CH₂)₂P⁺), 25.2 (CH₂(CH₂)₈P⁺), 28.0 (CH₂(CH₂)₇P⁺), 28.6 (CH₂(CH₂)₂CH₂(CH₂)₃P⁺), 28.7 ((CH₂)₂(CH₂)₄P⁺), 29.7 (*d*, *J*_{CP} = 16.4 Hz, CH₂CH₂P⁺), 36.3 (CH₂(CH₂)₉P⁺), 107.9 (C(2)), 110.3 (C(6)), 115.1 (C(5)), 118.6 (*d*, *J*_{CP} = 85.6 Hz, 3 × C(1')), 130.2 (*d*, *J*_{CP} = 12.4 Hz, 3 × C(3') and 3 × C(5')), 131.5 (C(1)), 133.6 (*d*, *J*_{CP} = 10.1 Hz, 3 × C(2') and 3 × C(6')), 134.9 (*d*, *J*_{CP} = 2.9 Hz, 3 × C(4')), 141.0 (C(4)), 144.8 (C(3)), 170.2 (CO).

(11-((3,4,5-trihydroxyphenyl)amino)11-oxoundecyl)triphenylphosphonium bromide (11f). Procedure D1. η = 93 %. ¹H NMR (DMSO *d*₆): δ = 1.12 – 1.32 (10H, *m*, (CH₂)₅(CH₂)₂P⁺), 1.37 – 1.58 (6H, *m*, (CH₂)₂(CH₂)₅CH₂CH₂P⁺), 2.19 (2H, *t*, *J* = 7.3 Hz, CH₂(CH₂)₉P⁺), 3.49 – 3.63 (2H, *m*, CH₂P⁺), 6.61 (2H, H(2) and H(6)), 7.71 – 7.94 (15H, *m*, PPh₃), 9.37 (1H, *s*, NH). ¹³C NMR (DMSO *d*₆): δ = 20.2 (*d*, *J*_{CP} = 49.7 Hz, CH₂P⁺), 21.7 (*d*, *J*_{CP} = 4.2 Hz, CH₂(CH₂)₂P⁺), 25.3 (CH₂(CH₂)₈P⁺), 28.0 (CH₂(CH₂)₇P⁺), 28.6 (CH₂(CH₂)₆P⁺), 28.7 (CH₂CH₂CH₂(CH₂)₃P⁺), 28.8 (CH₂(CH₂)₄P⁺), 29.7 (*d*, *J*_{CP} = 16.3 Hz, CH₂CH₂P⁺), 36.4 (CH₂(CH₂)₉P⁺), 99.0 (C(2) and C(6)), 118.6 (*d*, *J*_{CP} = 85.6 Hz, 3 × C(1')), 128.8 (C(4)), 130.2 (*d*, *J*_{CP} = 12.4 Hz, 3 × C(3') and 3 × C(5')), 130.9 (C(1)), 133.6 (*d*, *J*_{CP} = 10.1 Hz, 3 × C(2') and 3 × C(6')), 134.9 (*d*, *J*_{CP} = 2.8 Hz, 3 × C(4')), 145.8 (C(3) and C(5)), 170.4 (CO).

Pharmacology

Antimicrobial screenings. All screening was performed as two replicas (*n* = 2) on different assay plates, but from single plating and performed in a single screening experiment (microbial incubation). In addition, two values were used as quality controls for individual plates: Z'-Factor = [1 - (3*(sd(NegCtrl) + sd(PosCtrl)))/(average(PosCtrl) - average(NegCtrl))] [22] and Standard Antibiotic controls at different concentrations (>MIC and < MIC). The plate passes the quality control if Z'-Factor > 0.4 and Standards were active and inactive at highest and lowest concentrations, respectively (data not supplied).

Standards and sample preparation. Colistin and vancomycin were used as positive bacterial inhibitor references for Gram-negative and Gram-positive bacteria, respectively. Fluconazole was used as a positive fungal inhibitor reference for *C. albicans* and *C. neoformans var. grubii*. Tamoxifen and melittin were used as positive references for cytotoxicity and hemolysis, respectively.

Stock solutions of compounds were prepared in DMSO. Samples were prepared in DMSO and water to a final testing concentration of 32 μg/mL in 384-well, non-binding surface plate (NBS) for each bacterial/fungal strain, and in duplicate (*n* = 2), and keeping the final DMSO concentration to a maximum of 1 % DMSO. The sample preparation was done using liquid handling robots.

Antimicrobial screening. *In vitro* antibacterial and antifungal activities were determined on the basis of MIC values. Stock solutions of the test compounds were prepared in DMSO. Compounds were plated as a 2-fold dose response from 32 to 0.25 µg/mL (or 20 to 0.156 µM), with a maximum concentration of DMSO of 0.5 %. The determination of MIC values was performed following the Clinical & Laboratory Standards Institute (CLSI) guidelines [23], identifying the lowest concentration at which full inhibition of the bacteria or fungi has been detected. Full inhibition of growth has been defined at ≤ 20% growth (or > 80% inhibition), and concentrations have only been selected if the next highest concentration displayed full inhibition (i.e. 80–100%) as well (eliminating 'singlet' active concentration).

Evaluation of antibacterial activity

All bacteria (*S. aureus* ATCC 43300; *E. coli* ATCC 25922, *K. pneumoniae* ATCC 70060, *P. aeruginosa* ATCC 27853, *A. baumannii* ATCC 19606) were cultured in cation-adjusted Mueller Hinton broth (CAMHB) at 37 °C overnight. A sample of each culture was then diluted 40-fold in fresh broth and incubated at 37 °C for 1.5–3 h. The resultant mid-log phase cultures were diluted (CFU/mL measured by OD_{600 nm}), then added to each well of the compound containing plates, giving a cell density of 5 × 10⁵ CFU/mL and a total volume of 50 µL. All the plates were covered and incubated at 37 °C for 18 h without shaking.

The growth inhibition of all bacteria was determined measuring absorbance at 600 nm (OD₆₀₀), using a Tecan M1000 Pro monochromator plate reader. The percentage of growth inhibition was calculated for each well, using the negative control (media only) and positive control (bacteria without inhibitors) on the same plate as references. The significance of the inhibition values was determined by modified Z-scores, calculated using the median and MAD of the samples (no controls) on the same plate [24]. Samples with inhibition value above 80% and Z-Score above 2.5 for either replicate (*n* = 2 on different plates) were classed as actives.

Evaluation of antifungal activity.

Fungi strains (*C. albicans* ATCC 90028 and *C. neoformans* var. *grubii* H99 ATCC 208821) were cultured for 3 days on Yeast Extract-Peptone Dextrose (YPD) agar at 30 °C. A yeast suspension of 1 × 10⁶ to 5 × 10⁶ CFU/mL (as determined by OD_{530 nm}) was prepared from five colonies. The suspension was subsequently diluted and added to each well of the compound-containing plates giving a final cell density of fungi suspension of 2.5 × 10³ CFU/mL and a total volume of 50 µL. All plates were covered and incubated at 35 °C for 24 h without shaking.

The growth inhibition of *C. albicans* was determined by measuring the absorbance at 530 nm (OD_{530 nm}). The growth inhibition of *C. neoformans* var. *grubii* was determined by measuring the difference in absorbance between 600 and 570 nm (OD₆₀₀₋₅₇₀), following the addition of resazurin (0.001 % final concentration) and incubation at 35 °C for additional 2 h. The absorbance was measured using a Biotek Synergy HTX plate reader. The percentage of growth inhibition was calculated for each well, using the negative control (media only) and positive control (bacteria without inhibitors) on the same plate as references. The significance of the inhibition values was determined by modified Z-scores, calculated using the median and MAD of the samples (no controls) on the same plate. Samples with inhibition value above 80% and Z-Score above 2.5 for either replicate (*n* = 2 on different plates) were classed as actives.

Evaluation of cytotoxicity profile

HEK293 cells (ATCC CRL-1573) were counted manually in a Neubauer haemocytometer and then plated in the 384-well plates

containing the compounds to give a density of 5000 cells/well in a final volume of 50 µL. DMEM supplemented with 10% FBS was used as growth media and the cells were incubated together with the compounds for 20 h at 37 °C in 5% CO₂.

Growth inhibition of HEK293 cells was determined measuring fluorescence at ex:530/10 nm and em:590/10 nm (F_{560/590}), after the addition of resazurin (25 µg/mL final concentration) and incubation at 37 °C and 5% CO₂, for additional 3 h. The fluorescence was measured using a Tecan M1000 Pro monochromator plate reader. The percentage of growth inhibition was calculated for each well, using the negative control (media only) and positive control (cell culture without inhibitors) on the same plate as references. CC₅₀ values were obtained from dose-response curves, with variable values for bottom, top and slope. The curve fitting was implemented using Pipeline Pilot's dose-response component.

Evaluation of haemolytic activity

The use of human blood (sourced from LifeBlood) for hemolysis assays was approved by the University of Queensland Institutional Human Research Ethics Committee, Approval Number 2020001239.

Human whole blood was washed three times with 3 volumes of 0.9% NaCl and then resuspended in same to a concentration of 0.5 × 10⁸ cells/mL, as determined by manual cell count in a Neubauer haemocytometer. The washed cells were then added to the 384-well compound-containing plates for a final volume of 50 µL. After a 10 min shake on a plate shaker, the plates were incubated for 1 h at 37 °C. After incubation, the plates were centrifuged at 1000 × g for 10 min to pellet cells and debris, 25 µL of the supernatant was transferred to a polystyrene 384-well assay plate. Haemolysis was determined by measuring the supernatant absorbance at 405 nm (OD₄₀₅). The absorbance was measured using a M1000 Pro monochromator plate reader (Tecan Trading AG, Switzerland) [25].

The determination of HC₁₀ values were performed values were obtained from dose-response curves, with variable values for bottom, top and slope. The curve fitting was implemented using Pipeline Pilot's dose-response component. The curve fitting resulted in HC₅₀ values, which are converted into HC₁₀ using Equation (1).

$$HC_{10} = HC_{50} \times \left(\frac{10}{90} \right)^{\frac{1}{\text{slope}}} \quad (1)$$

Evaluation of the antibacterial mechanism of action

The evaluation of the antibacterial mechanism of action of the selected compounds was performed with *S. aureus* XU212 (Clinical isolate; TetK efflux pump overexpresser; MRSA strain [26]).

Determination of minimum inhibitory concentration and minimum bactericidal concentration

The determination of MIC and MBC values of compounds **5 m** and **5 n** was performed by the broth microdilution method according to Borges *et al.* [27]. Briefly, an overnight bacterial culture (16–18 h) grown in flasks containing Mueller-Hinton broth (MHB; Oxoid, England) was adjusted to an optical density (OD) of 0.132 ± 0.02 (λ = 600 nm) with fresh MHB. Then, 96-well polystyrene microtiter plates were filled with 20 µL of solutions of the test compounds at different concentrations (final concentrations: 0.0625–32 µg/mL) and 180 µL of bacterial suspension. Positive controls include bacterial suspension without compounds and with DMSO (at 10 %, v/v). After 24 h incubation at 37 °C and 150 rpm, the bacterial growth was analysed by measuring the absorbance at 600 nm in a microtiter plate reader (FLUOstar Omega; BMG LABTECH, Germany). The MIC value was defined as the lowest concentration that prevented the bacterial growth.

After MIC determination, 10 μ L of bacterial suspension was directly removed from the wells containing the test compound at concentrations equal to and above the MIC and placed out on MH agar. Plates were incubated at 37 °C for 24 h and the growth was visually inspected. The MBC was recorded as the lowest concentration in which total growth inhibition in solid medium was observed.

Evaluation of cytoplasmic membrane integrity

The effects of compounds **5 m** and **5 n** on the cytoplasmic membrane integrity of *S. aureus* XU212 were evaluated. After exposure with the test compounds at different concentrations ($\frac{1}{2}$ MIC, MIC and $2 \times$ MIC) for 1 h, the following measurements were performed: (a) zeta potentials, (b) propidium iodide (PI) uptake and (c) intracellular K^+ release. All tests were performed with a minimum of two independent repeats.

- The zeta potential was determined using a Nano Zetasizer Pro (Malvern Instrument, UK) by applying an electric field across the bacterial suspensions under specific pH and salt concentrations [27].
- The Live/Dead BacLight™ kit (Invitrogen-Molecular Probes, USA) was applied to assess membrane integrity by selective stain exclusion [27]. The kit includes two nucleic acid-binding stains, SYTO 9 and PI. Green fluorescing SYTO 9™ is able to enter all cells, whereas red fluorescing PI enters only in cells with damaged cytoplasmic membranes. Thus, bacteria with intact cell membranes stain fluorescent green, whereas bacteria with damaged membranes stain fluorescent red.
- Flame emission and atomic absorption spectroscopy (GBC AAS 932plus device; GBC Avante 1.33 software) were used for K^+ titration in bacterial suspensions according to Borges et al. [27].

Statistical analysis

The data obtained are expressed as mean \pm standard deviation of at least two independent experiments ($n = 2$). All statistical analyses were performed using GraphPad PRISM version 6 for Windows. One-way ANOVA with Bonferroni test was performed for data assuming a normal distribution. Statistical analysis was based on a confidence level of $\geq 95\%$, where $p < 0.05$ was considered statistically significant.

Results and discussion

Chemistry

The phytochemical-based TPP⁺ conjugates **5a-x** and **11a-f** (Fig. 2) were obtained following three- or four-step synthetic strategies presented in Schemes 1-3. Structurally, these tripartite compounds contain a phenolic ring, a carboxamide group and a TPP⁺ cation and, with all the moieties linked through different inserts (Fig. 1). Structural diversity was attained by modifying the substitution pattern of the aromatic ring, the type of the spacer between the carboxamide function and the aromatic ring, and the length of the alkyl linker between the carboxamide and the TPP⁺ cation. The aromatic substitution pattern included di- (catechol) or trihydroxyl (pyrogallol) systems that were directly bound to a carboxamide group (Ph-CONH-) or through methylene ($n_1 = \text{Ph-CH}_2-$), ethylene ($n_1 = \text{Ph-H}_2\text{C-CH}_2-$) or vinyl ($n_1 = \text{Ph-HC}=\text{CH-}$) spacers (Fig. 2). Finally, six- ($n_2 = 1$), eight- ($n_2 = 2$) and ten-carbon ($n_2 = 3$) alkyl linkers were used to connect the carboxamide function to the TPP⁺ cation. For benzoic acid derivatives, a *retro*-amide group (Ph-NHCO-) was also considered.

The synthesis of compounds **5a-t** followed the strategies previously described by our group [18–21] and depicted in Scheme 1. Briefly, hydroxyalkylamides **2a-t** were obtained by reacting the carboxylic acids **1a-h** with the appropriate hydroxyalkylamines using phosphorus oxychloride (Scheme 1, step a) or ethyl chloroformate (Scheme 1, step b) as coupling agents. The hydroxyalkyl groups of the intermediates **2a-t** were then activated through generation of the corresponding halides (Scheme 1, step c) or mesylates (Scheme 1, step d). After reaction with triphenylphosphine (TPP), salts **4a-t** were obtained (Scheme 1, step e). Subsequent *O*-demethylation of compounds **4a-t** with boron tribromide solution yielded the final phenolic compounds **5a-t**.

A different synthetic strategy was developed to obtain compounds **5u-x** (Scheme 2), allowing to reduce hands-on time and to streamline the purification steps. First, aminoalkyltriphenylphosphonium salt **7** was synthesized by heating TPP with *N*-(8-bromooctyl)phthalimide, followed by the cleavage of the phthalimide ring with butylamine (Scheme 2, step a). Then, amidation reaction between carboxylic acids **1c-f** and compound **7**, using ethyl chloroformate as coupling agent, yielded the intermediates **4u-x** (Scheme 2, step b). Finally, an *O*-demethylation reaction with boron tribromide solution was performed to obtain final phenolic derivatives **5u-x** (Scheme 2, step c).

Compounds **11a-f** were synthesized by the three-step synthetic strategy depicted in Scheme 3. The first step consisted of the obtention of carboxyalkyltriphenylphosphonium salts **9a-c** by heating TPP with the appropriate bromoalkylcarboxylic acid (Scheme 3, step a). Then, ethyl chloroformate-mediated amidations between compounds **9a-c** and amines **1i-j** yielded compounds **10a-f** (Scheme 3, step b). Finally, compounds **11a-f** were obtained by *O*-demethylation of compounds **10a-f**. Compounds **10b**, **10d** and **10f** were treated with boron tribromide solution to afford the pyrogallol derivatives **11b**, **11d** and **11f**, respectively (Scheme 3, step c). Compounds **10a**, **10c** and **10e** were refluxed with boron tribromide dimethyl sulfide complex to obtain catechols **11a**, **11c** and **11e**, respectively (Scheme 3, step d).

Antimicrobial screening

Following the synthesis of phytochemical-based TPP⁺ conjugates **5a-x** and **11a-f**, a preliminary high throughput screening of their antimicrobial activity was performed. All compounds were screened by the Community for Open Antimicrobial Drug Discovery (CO-ADD) against a key panel of drug-resistant bacterial strains, which include the Gram-positive methicillin-resistant *S. aureus* (MRSA) and different Gram-negative bacteria (*E. coli*, *K. pneumoniae*, *P. aeruginosa*, *A. baumannii*) and fungi (*C. albicans* and *C. neoformans* var. *grubii*) [28]. The minimum inhibitory concentrations (MIC) of compounds against growing planktonic cells were determined using the broth microdilution method. Vancomycin and colistin were used as positive references for Gram-positive and Gram-negative bacteria, respectively. Fluconazole was used as a positive reference for *C. albicans* and *C. neoformans* (Table 1). To rationalize the data, compounds were divided into five series (A-E).

Cytotoxicity and haemolytic screening

The cytotoxicity in human embryonic kidney cells (HEK293) and haemolytic activity in human red blood cells (RBC) of the most promising phytochemical-based TPP⁺ conjugates (compounds **5e**, **5f**, **5i**, **5j**, **5 m**, **5 n**, **5 p**, **5 r**, **5 s**, **5 t**, **5 x**, **11 d**, **11 e** and **11 f**) were evaluated. The results obtained are expressed as concentration at 50 % cytotoxicity (CC₅₀) and concentration at 10 % haemolytic activity (HC₁₀), respectively (Table 2). Tamoxifen and melittin were used as a positive cytotoxicity and haemolytic references, respectively.

Table 1

MIC values ($\mu\text{g/mL}$) of the phytochemical-based TPP⁺ conjugates **5a-x**, **11a-f** and reference antibiotics against the selected microorganisms.

Series	Compound	R	n ₂	MIC						
				<i>S. aureus</i>	<i>E. coli</i>	<i>K. pneumoniae</i>	<i>P. aeruginosa</i>	<i>A. baumannii</i>	<i>C. albicans</i>	<i>C. neoformans</i>
A	5a	H	1	>32	>32	>32	>32	>32	>32	>32
	5b	OH	1	>32	>32	>32	>32	>32	>32	>32
	5c	H	2	>32	>32	>32	>32	>32	>32	>32
	5d	OH	2	32	>32	>32	>32	>32	>32	>32
	5e	H	3	8	>32	>32	>32	>32	>32	>32
	5f	OH	3	16	>32	>32	>32	>32	>32	>32
B	5g	H	1	>32	>32	>32	>32	>32	>32	>32
	5h	OH	1	>32	>32	>32	>32	>32	>32	>32
	5u	H	2	>32	>32	>32	>32	>32	>32	>32
	5v	OH	2	>32	>32	>32	>32	>32	>32	>32
	5i	H	3	8	>32	>32	>32	>32	32	>32
	5j	OH	3	8	>32	>32	>32	>32	>32	32
C	5k	H	1	32	>32	>32	>32	>32	>32	>32
	5l	OH	1	>32	>32	>32	>32	>32	>32	>32
	5w	H	2	>32	>32	>32	>32	>32	>32	>32
	5x	OH	2	8	>32	>32	>32	>32	>32	>32
	5m	H	3	≤ 0.25	>32	>32	>32	>32	>32	>32
	5n	OH	3	≤ 0.25	>32	>32	>32	>32	>32	>32
D	5o	H	1	>32	>32	>32	>32	>32	>32	>32
	5p	OH	1	>32	>32	>32	>32	>32	>32	16
	5q	H	2	>32	>32	>32	>32	>32	>32	>32
	5r	OH	2	32	>32	>32	>32	>32	>32	16
	5s	H	3	8	>32	>32	>32	>32	16	16
	5t	OH	3	16	>32	>32	>32	>32	16	4
E	11a	H	1	>32	>32	>32	>32	>32	32	>32
	11b	OH	1	32	>32	>32	>32	>32	>32	32
	11c	H	2	>32	>32	>32	>32	>32	>32	>32
	11d	OH	2	16	>32	>32	>32	>32	>32	8
	11e	H	3	16	>32	>32	>32	>32	32	>32
	11f	OH	3	2	>32	>32	>32	>32	8	4
	Colistin	—	—	>32	0.125	0.25	0.25	0.25	n.d.	n.d.
	Vancomycin	—	—	1	>32	>32	>32	>32	n.d.	n.d.
	Fluconazole	—	—	n.d.	n.d.	n.d.	n.d.	n.d.	0.125	8

Standard strains: *S. aureus* ATCC 43300; *E. coli* ATCC 25922; *K. pneumoniae* ATCC 70060; *P. aeruginosa* ATCC 27853; *A. baumannii* ATCC 19606; *C. albicans* ATCC 90028; and *C. neoformans* var. *grubii* H99 ATCC 208821.

n.d.: not determined.

Structure-activity-toxicity relationships.

From the preliminary data obtained (Tables 1 and 2), a structure-activity-toxicity analysis was performed. In general, phytochemical-based TPP⁺ conjugates acted as moderate or even potent antimicrobial agents. Remarkably, while the benzoyl, phenylacetyl and dihydrocinnamoyl derivatives endowed with antimicrobial activity were selective for *S. aureus*, cinnamoyl and phenylamide derivatives also presented antifungal activity against *C. albicans* and *C. neoformans* var. *grubii* (Table 1).

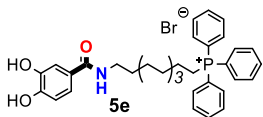
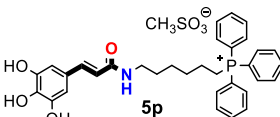
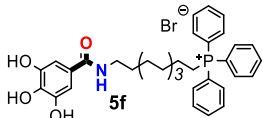
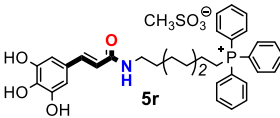
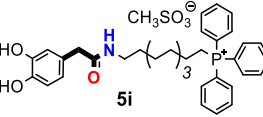
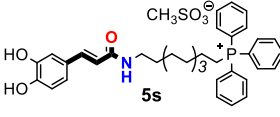
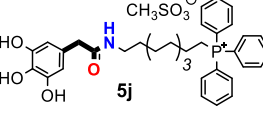
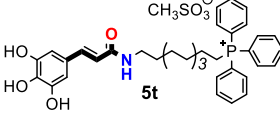
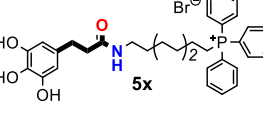
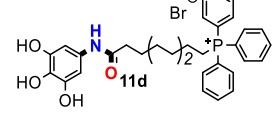
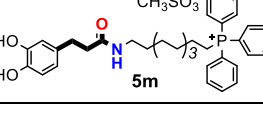
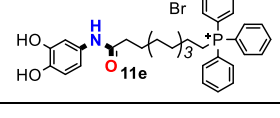
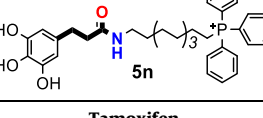
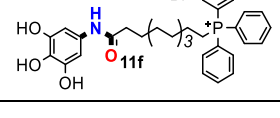
A correlation between the length of the alkyl linker and the antibacterial activity against *S. aureus* was observed. While all compounds containing a ten-carbon alkyl linker acted as antibacterial agents, only two compounds bearing an eight-carbon alkyl linker (compounds **5x** and **11d**) were active towards *S. aureus*, presenting higher MIC values than the ten carbon counterparts (compounds **5n** and **11f**, respectively).

Compared with benzoic acid derivatives (compounds **5d**, **5e** and **5f**), the antibacterial activity against *S. aureus* was enhanced with the incorporation of methylene (compounds **5v**, **5i** and **5j**) and ethylene spacers (compounds **5x**, **5m** and **5n**) between the phenolic ring and carboxamide group. Indeed, dihydrocinnamic acid derivatives **5m** and **5n** were the most potent antibacterial agents of the series, showing MIC values towards *S. aureus* below 0.25 $\mu\text{g/mL}$. Compounds bearing a cinnamoyl moiety (**5r**, **5s** and **5t**) exhibited higher MIC values towards *S. aureus* than the related dihydrocinnamic acid derivatives (compounds **5x**, **5m** and **5n**). Therefore, the low rigidity of the spacer

between the carboxamide group and the phenolic ring seems to be critical for effective antibacterial activity against *S. aureus*. In addition, given the lower or absent antibacterial activity of dihydrocinnamic acid derivatives with six-carbon (compounds **5k** and **5l**) or 8-carbon (compounds **5w** and **5x**), the synergism between the low rigidity of the ethylene spacer and the longer alkyl linker may be responsible for the high potency of compounds **5m** and **5n**. Phenyl amide derivatives **11b**, **11d** and **11f** displayed lower MIC values towards *S. aureus* than the related benzoic acid derivatives (compounds **5b**, **5d** and **5f**), indicating that the presence of a retro carboxamide group improves the antibacterial activity of TPP⁺ conjugates containing a pyrogallol moiety.

A direct correlation between longer alkyl linkers and low MIC values was also observed for *C. albicans* and *C. neoformans* var. *grubii*. Only compounds containing a ten-carbon alkyl linker (compounds **5s**, **5t** and **11f**) were active towards *C. albicans*, with the 3,4,5-trihydroxyphenylamide derivative **11f** exhibiting the lowest MIC value. Similarly, compounds **5t** and **11f** presented lower MIC values towards *C. neoformans* var. *grubii* than the related analogues with eight (**5r** and **11d**, respectively) or six-carbon alkyl linkers (**5p** and **11b**, respectively). The substitution pattern of the aromatic ring also influenced the antifungal activity against *C. neoformans* var. *grubii*. Except for compound **5s**, which contains a catechol group, only compounds with a pyrogallol moiety (compounds **5p**, **5r**, **5t**, **11d** and **11f**) were active against *C. neoformans* var. *grubii*.

Table 2Cytotoxicity in HEK293 cells (CC₅₀ in µg/mL) and haemolytic activity in RBC (HC₁₀ in µg/mL) of the most promising phytochemical-based TPP⁺ conjugates.

Compound	HEK293 (CC ₅₀) ^a	RBC (HC ₁₀) ^b	Compound	HEK293 (CC ₅₀) ^a	RBC (HC ₁₀) ^b
	9.07	>32		>32	>32
	>32	>32		>32	>32
	31.2	>32		10.7	11.9
	>32	>32		>32	6.0
	>32	>32		>32	>32
	>32	>32		22.4	>32
	>32	>32		>32	11.8
Tamoxifen	9	—			
Mellitin	—	2.7			

^a CC₅₀: concentration at 50 % cytotoxicity in human embryonic kidney (HEK-293) cells. ^bHC₁₀: concentration at 10% haemolytic activity in human red blood (RBC) cells.

From the data obtained in the evaluation of the compounds' cytotoxicity in HEK293 cells (Table 2), it was concluded that most of the bioactive TPP⁺ conjugates did not exhibit cytotoxic effects; only compounds **5e**, **5i**, **5s** and **11e** displayed CC₅₀ values below 32 µg/mL. All the mentioned compounds contain a catechol ring and a ten-carbon alkyl linker in their structure. Thus, the cytotoxicity observed may result from the combination of injurious effects induced by both structural components. Indeed, catechols can be oxidized into the corresponding *ortho*-quinones, which in turn can react with cellular nucleophiles or generate reactive species by redox-cycling processes [29]. Additionally, more hydrophobic TPP⁺ conjugates may negatively affect due to the higher affinity to biological membranes [30]. The CC₅₀ value of benzoyl derivative **5e** was similar to cinnamic acid derivative **5s** and lower than phenyl acetyl derivative **5i** and retro carboxamide **11e** (compound **5e**: CC₅₀ = 9.07 µg/mL; compound **5i**: CC₅₀ = 31.2 µg/mL; compound **5s**: CC₅₀ = 10.7 µg/mL; compound **11e**: CC₅₀ = 22.4 µg/mL). Interestingly, none of the dihydrocinnamic acid derivatives exhibited cytotoxic effects at concentrations below 32 µg/mL. Thus, the presence of an ethylene spacer between the phenolic ring and the amide group was associated with safe cytotoxicity profiles. The presence of a methylene spacer and a retro carboxamide group

were also associated with decreased cytotoxicity. Conversely, the introduction of a vinyl spacer did not improve the cytotoxicity profile of catechol TPP⁺ conjugates.

The most promising TPP⁺ conjugates were also tested for their haemolytic activity against human RBC (Table 2). The data obtained showed that, except for cinnamoyl and phenylamide derivatives with ten-carbon alkyl linkers (compounds **5s**, **5t** and **11f**), most compounds did not show haemolytic effects.

Based on the data obtained so far, we decided to continue our studies with the dihydrocinnamic acid derivatives **5m** and **5n** (Fig. 3). The selected compounds exhibited potent and selective antimicrobial activity towards *S. aureus* ATCC 43300 and were safe at concentrations below 32 µg/mL.

Antibacterial mechanism studies

To investigate the possible antibacterial mechanism of action of dihydrocinnamic acid derivatives **5m** and **5n**, several bacterial physiological indices were evaluated. These include MIC, minimum bactericidal concentration (MBC), surface charge, propidium iodide (PI) uptake and intracellular K⁺ release.

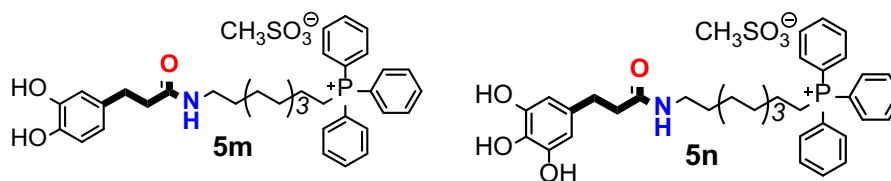


Fig. 3. Chemical structures of phytochemical-based TPP⁺ conjugates selected to unravel the antibacterial mechanism of action.

MIC and MBC determination

We first determined the inhibitory and bactericidal properties of each compound against *S. aureus* (XU212), a clinical isolate with known resistant profile (including TetK efflux pump and resistance to methicillin) and remarkable antibiotic resistance in comparison to other clinical isolates and collection strains of *S. aureus* [31].

The MIC and MBC values of the selected dihydrocinnamic acid derivatives are summarized in Tables 3. A MIC value of 16 µg/mL was obtained for both compounds (**5 m** and **5n**) against *S. aureus* (XU212). However, compound **5 m** displayed higher bactericidal activity. While compound **5 m** presented an MBC of 32 µg/mL, no MBC was obtained with compound **5n** at the maximum concentration tested (32 µg/mL).

Alterations in the surface charge

Following the determination of the compounds' antibacterial activity on *S. aureus* (XU212), we characterized their effects by evaluating surface charge alterations and cytoplasmic membrane disruption. To induce bacterial growth inhibition or even cell death, a compound needs first to interact with the cell surface and eventually reach the intracellular content.

The cell envelope of bacteria is a complex, dynamic and multi-layered structure, which serves as the first barrier against external stresses, toxic substances and host-immune defenses. In Gram-positive bacteria, the cell envelope is primarily composed of peptidoglycan, teichoic acids (TAs) and a variety of proteins, as well as polysaccharides and phospholipids. The lipid bilayer contains a large amount of cardiolipin and phosphatidylglycerol, being the lysyl type the predominant membrane lipid in *S. aureus*. The membrane play a key role in cellular integrity and in bacterial viability, being vital to maintain cellular homeostasis [32,33].

A very relevant factor related with microbial stability/equilibrium and antibacterial resistance is the charge of the cell surface. Under physiological conditions, bacterial cells (Gram-negative or Gram-positive) usually have a negative surface charge due to the

presence of anionic groups (e.g. carboxylic acid and phosphate) in their walls/membranes. This property varies within the species and can be influenced by several external conditions that can disturb lipid composition, such as culture age, ionic strength, temperature and pH [27,34]. In Gram-positive bacteria, the anionic membrane phospholipids and the phosphoryl groups located in the TAs tails of the cell wall (both wall teichoic acids (WTA) and lipoteichoic acids (LTA)) contribute to the negative surface charge [35].

To investigate whether the surface charge of *S. aureus* (XU212) is affected by compounds **5 m** and **5n**, the zeta potentials were measured (Table 4).

The results showed that, in the absence of the compounds, *S. aureus* (XU212) exhibited a negative potential (cells: ~ -25 mV; cells + DMSO: ~ -21 mV). When exposed to compounds **5 m** and **5n**, a small shift to less negative values was observed. Since the compounds tested contain a TPP⁺ cation, they can interact with the negatively charged TAs from bacterial cell wall through electrostatic interactions. These results suggest that the negatively charged phosphate group of WTA and LTA can attract the positively charged TPP⁺ group of compounds **5 m** and **5n**.

The high binding affinity between the compounds and the bacterial cell wall may promote the compounds' access to the cytoplasmic membrane, being capable of traversing from outside to the internal environment and thus exert its antimicrobial effects [35]. However, although TAs have been associated with cation binding (such as the compounds in study), some entrapment or ladder effect along the route to the plasma membrane may also occur [35]. For instance, the interaction of cationic antimicrobial peptides with peptidoglycans present in the cell wall seems to contribute to reduced antimicrobial activity. Moreover, the interaction with TAs, particularly LTA, may affect the concentration of compounds in the cytoplasmic required to promote positive membrane destabilization and/or killing [35]. In fact, in *S. aureus*, the positive charges of lysyl-phosphatidylglycerol from the cytoplasmic membrane are important in the repulsion of positively charged antibiotics or antibiotic-metal complexes. Therefore, the modulation of the negative charge density or cation homeostasis of the cell envelope, for instance by lysinylation of phosphatidylglycerol and D-alanylation of TA, can be a relevant aspect in the infection treatment. WTA is one of the main factors related to methicillin resistance in *S. aureus*, and its absence contribute to a greater

Table 3

MIC and MBC values (µg/mL) of compounds **5 m** and **5n** for *S. aureus* XU212.

Compound	MIC (µg/mL)	MBC (µg/mL)
5 m	16	32
5n	16	> 32

Table 4

Zeta potential (mV) values of *S. aureus* XU212 before (cells and cells + DMSO) and after contact with compounds **5 m** and **5n** at different concentrations (½ MIC, MIC and 2 × MIC) for 1 h.

Zeta Potential (mV)							
Controls		5 m			5n		
Cells	Cells + DMSO	½ MIC ^a	MIC ^a	2 × MIC ^a	½ MIC ^a	MIC ^a	2 × MIC ^a
-25.06 ± 6.10	-21.65 ± 4.58	-19.22 ± 1.22	-18.91 ± 0.84	-19.11 ± 0.95	-18.14 ± 0.31	-18.35 ± 0.50	-18.38 ± 0.25

^a ½ MIC = 8 µg/mL; MIC = 16 µg/mL; 2 × MIC = 32 µg/mL.

susceptibility to this antibiotic [32]. The few available studies with SKQ1 suggest that its antibacterial mechanism of action may involve the neutralization of the bacterial membrane potential [16,17]. Thus, the antimicrobial activity of compounds **5 m** and **5 n** may also result from surface charge effects.

Bacterial membrane integrity

The potential of the selected dihydrocinnamic acid derivatives to interfere with bacterial membrane integrity after 1 h exposure at different concentrations ($\frac{1}{2}$ MIC, MIC and $2 \times$ MIC;) was also analyzed. Cytoplasmic membrane permeabilization was studied to a certain extent by evaluating PI uptake through epifluorescence microscopy (Figs. 4 and 5). PI is a nucleic acid stain to which intact cell membranes are usually impermeable.

The results obtained demonstrated that, compared to control experiments (cells not exposed to tested compounds – 5.2% and cells exposed to solvent DMSO – 12.5%), only treatment with compound **5 n** inflicted damage (increased PI uptake) on the cytoplasmic membrane of *S. aureus* (XU212) (Fig. 4). The effects observed for compound **5 n** were dose-dependent, with the percentage of cells with damaged membranes increasing from 26.1% (at $\frac{1}{2}$ MIC) to 44.7% (at $2 \times$ MIC) ($p < 0.05$). Interestingly, some morphological “deformation” of the bacterial cells, denoted by surface irregularities and broken form, was observed. In fact, despite the low resolution of epifluorescence microscopy, it was possible to visualize a loss of the perfect spherical shape of the cell surface of native cells (without treatment).

The effects of compound **5 n** on the structure of bacterial cell membranes [36] may result from alterations in the rigidity and dynamics of phospholipid chains [37]. The induction of large pore formation in lipid membranes may also occur, as previously demonstrated for other phenolic compounds such as (-)-epigallocatechin gallate [38].

Given the low MIC/MBC values obtained for dihydrocinnamic derivatives **5 m** and **5 n** (Table 3), we expect more pronounced effects on membrane permeabilization experiments. However, since *S. aureus* XU212 cells were exposed to the test compounds for different periods in the determination of MIC/MBC values (24 h) and in the measurement of zeta potentials (1 h), we hypothesize that the inhibitory/killing effect is not immediate. In fact, it is plausible that the membrane disruption is time-dependent, result-

ing from a gradual compound accumulation within the cells. This is specifically evidenced in the epifluorescence images of 24 h Live/Dead membrane permeabilization assays, where a considerable number of cells with damaged membranes can be observed for both compounds at MIC and $2 \times$ MIC (Fig. 5).

Cytoplasmic leakage

In a work conducted by Pérez-Peinado *et al.* [39], they concluded that the mechanism of bacterial membrane disruption of cationic peptides involved three main stages: (1) initial peptide recruitment; (2) peptide accumulation; and (3) cell death by membrane disruption. They also showed that the antimicrobial activity only occurs when a threshold concentration on the bacterial surface is attained.

Since the cytoplasmic membrane of bacteria also acts as a barrier between the cytoplasm and the extracellular medium, the leakage of cytoplasmic material like ions provide a good indication on the membrane weakening. Indeed, K^+ leakage is considered one of the first indicators of membrane damage in microorganisms [40]. In this context, we monitored the bacterial release of K^+ after exposure to compounds **5 m** and **5 n** for 1 h. The results presented in Fig. 6 showed the occurrence of primary membranolytic events with compound **5 m** at $2 \times$ MIC ($2.12 \pm 0.55 \mu\text{g/mL}$) and with **5 n** at all concentrations tested ($\frac{1}{2}$ MIC = 1.80 ± 0.21 ; MIC = 2.13 ± 0.17 ; $2 \times$ MIC = 2.24 ± 0.34) ($P < 0.05$), corroborating the data obtained in PI uptake experiments (Fig. 4). The release of intracellular content may indicate the formation of a local pore in the phospholipid membranes and not just on its destabilization.

In summary, the data obtained so far indicate that dihydrocinnamic acid derivatives **5 m** and **5 n** exert their antibacterial activity by targeting mainly the bacterial surface. We hypothesize that the antimicrobial activity of compounds **5 m** and **5 n** may result from their interaction with cell surface components required for microbial growth and survival (e.g. peptidoglycan, TA, proteins and other critical biological macromolecules), accumulating on the cell membrane or forming a monolayer around the cell that changes the membrane potential and induce local rupture and/or pore formation. The results further propose that the antimicrobial action happens in a sequence of events, starting with a change of the membrane surface charge, followed by the disruption of the membrane integrity. A comparable mode of action was observed previ-

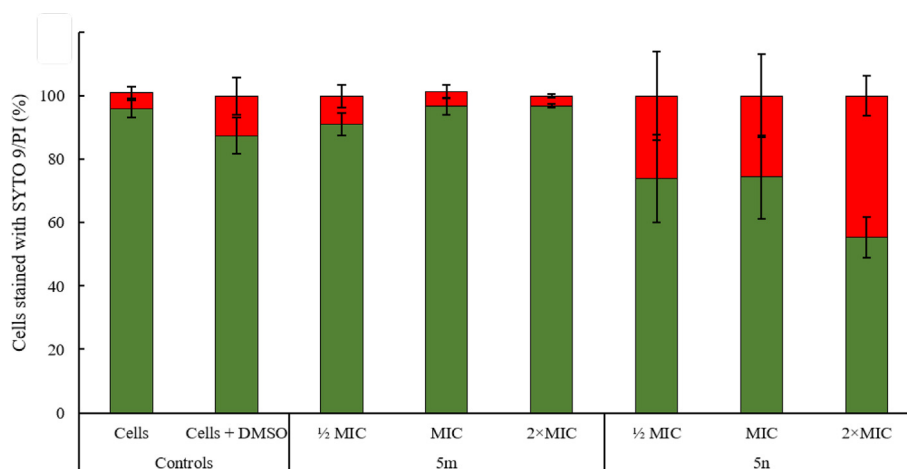


Fig. 4. Percentage of *S. aureus* XU212 cells stained with SYTO 9 (Intact cell membranes; ■) and PI (Damaged cell membranes; ■) after 1 h exposure to compounds **5 m** and **5 n** at different concentrations ($\frac{1}{2}$ MIC, MIC and $2 \times$ MIC). Results are expressed as mean values \pm standard deviation of at least two replicates ($n = 2$). Bars marked with * are statistically different from control (*S. aureus* XU212) cells not exposed to tested compounds – Cells + DMSO). One-way ANOVA with Bonferroni test was performed for data assuming a normal distribution. Statistical analysis was based on a confidence level of $\geq 95\%$, where $p < 0.05$ was considered statistically significant.

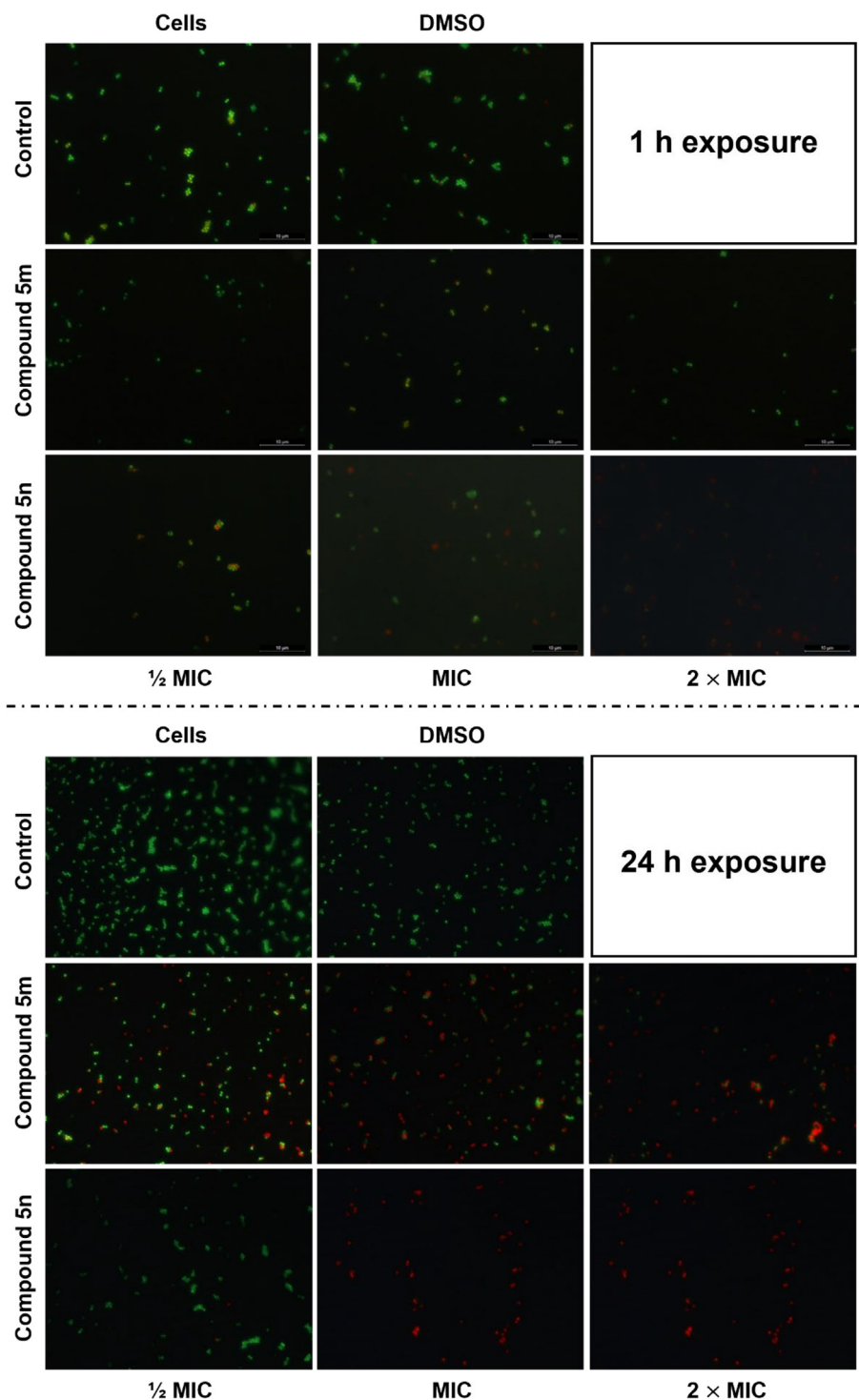


Fig. 5. Representative epifluorescence micrographs of *S. aureus* XU212 cells visualized using Live/Dead BacLight™ kit (SYTO 9 and PI). The *S. aureus* XU212 cells were treated with compounds **5 m** and **5 n** at different concentrations ($\frac{1}{2}$ MIC, MIC and $2 \times$ MIC) for 1 h and 24 h. Controls: no treatment (cells not exposed to tested compounds – Cells; cells exposed to DMSO solvent (at 10% v/v) – Cells + DMSO). Scale bar: 10 μ m.

ously when *S. aureus* was exposed to a hydroxycinnamic acid and a hydroxybenzoic acid [27].

Since some of the phytochemical-based TPP⁺ conjugates can remodel mitochondrial bioenergetics by modulating mitochondrial respiration [41,42], additional studies are envisioned to better understand their antibacterial mechanism of action. Like mito-

chondria, bacteria depend on an electrochemical gradient of protons across the cytoplasmic membrane, known as proton motive force, which drives crucial processes in bacteria [43]. Phytochemical-based TPP⁺ conjugates may also have protonophoric/ionophoric activity. The ionization of the phenol group ($pK_a > 8$) can occur in certain compartments [44,45] and may diffuse

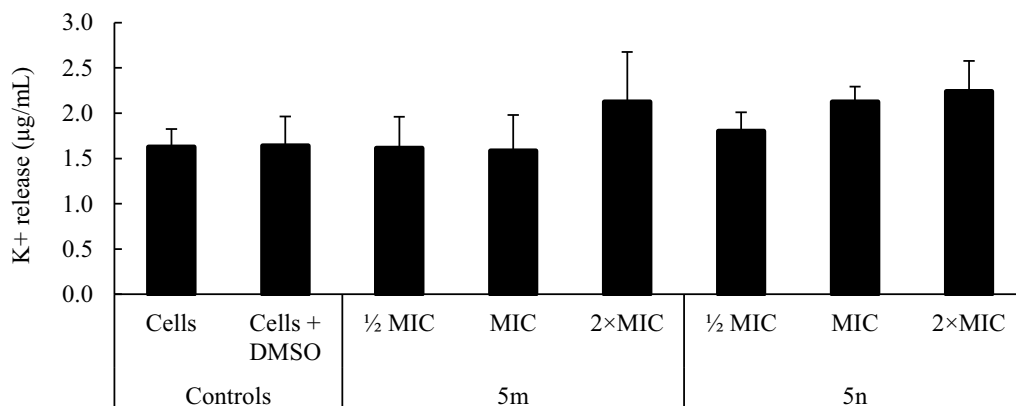


Fig. 6. K⁺ release (µg/mL) by *S. aureus* XU212 before (cells and cells + DMSO) and after exposure to compounds **5m** and **5n** at different concentrations (1/2 MIC, MIC and 2 × MIC) for 1 h. Results are presented as mean values ± standard deviation for at least two replicates ($n = 2$). One-way ANOVA with Bonferroni test was performed for data assuming a normal distribution. Statistical analysis was based on a confidence level of $\geq 95\%$, where $p < 0.05$ was considered statistically significant.

across the membranes, transport protons or other cations, and equilibrate/dissipate ionic gradients [46].

Conclusions

In this work, phytochemical-based TPP⁺ conjugates were successfully synthesized and screened towards different bacterial and fungal strains. From structure-activity-toxicity studies, it was concluded that the presence of a ten-carbon alkyl linker between the carboxamide group and the TPP⁺ cation enhances the antimicrobial activity of compounds. The incorporation of methylene and ethylene spacers improved the bioactivity and the safety of compounds while preserving their selectivity towards *S. aureus*. In contrast, the introduction of a vinyl spacer and the retroamide group endowed lipophilic TPP⁺ cations with antifungal activity, although it was also accompanied with cytotoxic and/or haemolytic effects. While no correlation was found between the substitution pattern of the phenolic ring and the bioactivity towards *S. aureus* and *C. albicans*, pyrogallol derivatives were more active towards *C. neoformans* var. *grubii* than catechols. The presence of a catechol group was associated with increased cytotoxicity, especially when combined with a ten-carbon alkyl linker. Based on the studies performed to unravel the antibacterial mechanism of action of TPP⁺ conjugates **5m** and **5n**, it was concluded that the lipophilic and cationic nature of these compounds are important features for cell wall interaction and penetration in *S. aureus*. Phytochemical-based TPP⁺ conjugates may access the bacterial cell membrane, promoting its destabilization through the disruption of the transmembrane potential and local rupture with leakage of important cytoplasmic constituents.

Overall, the data obtained provides valuable insights in the development of phytochemical-based TPP⁺ conjugates with antimicrobial activity and possibly to the discovery of a new class of antibiotics. Novel lead compounds can be optimized in a foreseeable future and translated into a drug candidate able to tackle MDR bacteria.

CRediT authorship contribution statement

Daniel Chavarria: Investigation, Data curation, Formal analysis, Writing – original draft. **Anabela Borges:** Investigation, Data curation, Formal analysis, Writing – original draft. **Sofia Benfeito:** Investigation. **Lisa Sequeira:** Investigation. **Marta Ribeiro:** Investigation. **Catarina Oliveira:** Investigation. **Fernanda Borges:** Conceptualization, Methodology, Funding acquisition, Project

administration, Resources, Supervision. **Manuel Simões:** Conceptualization, Methodology, Funding acquisition, Project administration, Resources, Supervision, Writing – review & editing. **Fernando Cagide:** Conceptualization, Methodology, Funding acquisition, Project administration, Resources, Supervision, Writing – review & editing.

Declaration of Competing Interest

The authors declare that they have no known competing financial interests or personal relationships that could have appeared to influence the work reported in this paper.

Acknowledgements

This work was funded by FEDER funds through the Operational Programme Competitiveness Factors–COMPETE and national funds by FCT – Foundation for Science and Technology under research grants (Grants PTDC/ASP-PES/28397/2017 - POCI-01-0145-FEDER-028397, UIDB/00081/2020 (CIQUP), LA/P/0056/2020 (IMS), LA/P/0045/2020 (ALiCE), UIDP/00511/2020 (LEPABE)). DC, FC, AB [CEECIND/00823/2021] thanks FCT, POPH, FEDER/COMPETE for their grants. SB grant is supported by PT-OPENSREEN–NORTE-01-0145-FEDER-085468 project. The authors thank CO-ADD (The Community for Open Antimicrobial Drug Discovery) not-for-profit initiative, funded by the Wellcome Trust (UK) and The University of Queensland (Australia) for performing the preliminary antimicrobial and toxicity screenings.

Appendix A. Supplementary data

Supplementary data to this article can be found online at <https://doi.org/10.1016/j.jare.2023.02.004>.

References

- [1] Rossiter SE, Fletcher MH, Wuest WM. Natural Products as Platforms to Overcome Antibiotic Resistance. *Chem Rev* 2017;117:12415–74. doi: <https://doi.org/10.1021/acs.chemrev.7b00283>.
- [2] Gunjal VB, Thakare R, Chopra S, Reddy DS. Teixobactin: A Paving Stone toward a New Class of Antibiotics?. *J Med Chem* 2020;63:12171–95. doi: <https://doi.org/10.1021/acs.jmedchem.0c00173>.
- [3] Lin B, Hung A, Li R, Barlow A, Singleton W, Matthyssen T, et al. Systematic comparison of activity and mechanism of antimicrobial peptides against nosocomial pathogens. *Eur J Med Chem* 2022;231. doi: <https://doi.org/10.1016/j.ejmech.2022.114135>.

- [4] Pisano MB, Kumar A, Medda R, Gatto G, Pal R, Fais A, et al. Antibacterial Activity and Molecular Docking Studies of a Selected Series of Hydroxy-3-arylcoumarins. *Molecules* 2019;24:2815. doi: <https://doi.org/10.3390/molecules24152815>.
- [5] Guo Y, Hou E, Wen T, Yan X, Han M, Bai LP, et al. Development of Membrane-Active Honokiol/Magnolol Amphiphiles as Potent Antibacterial Agents against Methicillin-Resistant *Staphylococcus aureus* (MRSA). *J Med Chem* 2021;64:12903–16. doi: <https://doi.org/10.1021/acs.jmedchem.1c01073>.
- [6] Linciano P, Cavalloro V, Martino E, Kirchmair J, Listro R, Rossi D, et al. Tackling Antimicrobial Resistance with Small Molecules Targeting LsrK: Challenges and Opportunities. *J Med Chem* 2020;63:15243–57. doi: <https://doi.org/10.1021/acs.jmedchem.0c01282>.
- [7] Li B, Ouyang X, Ba Z, Yang Y, Zhang J, Liu H, et al. Novel β -Hairpin Antimicrobial Peptides Containing the β -Turn Sequence of -RRRF- Having High Cell Selectivity and Low Incidence of Drug Resistance. *J Med Chem* 2022;65:5625–41. doi: <https://doi.org/10.1021/acs.jmedchem.1c02140>.
- [8] Heidtmann CV, Voukia F, Hansen LN, Sørensen SH, Urlund B, Nielsen S, et al. Discovery of a Potent Adenine-Benzyltriazolo-Pleuromutilin Conjugate with Pronounced Antibacterial Activity against MRSA. *J Med Chem* 2020;63:15693–708. doi: <https://doi.org/10.1021/acs.jmedchem.0c01328>.
- [9] Ermolaev VV, Arkhipova DM, Miluykov VA, Lyubina AP, Amerhanova SK, Kulik NV, et al. Sterically hindered quaternary phosphonium salts (QPS): Antimicrobial activity and hemolytic and cytotoxic properties. *Int J Mol Sci* 2022;23:86. doi: <https://doi.org/10.3390/ijms23010086>.
- [10] Xue Y, Xiao H, Zhang Y. Antimicrobial polymeric materials with quaternary ammonium and phosphonium salts. *Int J Mol Sci* 2015;16:3626–55. doi: <https://doi.org/10.3390/ijms16023626>.
- [11] Fu Y, Wang F, Sheng H, Xu M, Liang Y, Bian Y, et al. Enhanced antibacterial activity of magnetic biochar conjugated quaternary phosphonium salt. *Carbon* 2020;163:360–9. doi: <https://doi.org/10.1016/j.carbon.2020.03.010>.
- [12] Wessels S, Ingmer H. Modes of action of three disinfectant active substances: A review. *Regul Toxicol Pharmacol* 2013;67:456–67. doi: <https://doi.org/10.1016/j.yrtph.2013.09.006>.
- [13] Lei Q, Lai X, Zhang Y, Li Z, Li R, Zhang W, et al. PEGylated Bis-Quaternary Triphenyl-Phosphonium Tosylate Allows for Balanced Antibacterial Activity and Cytotoxicity. *ACS Appl Bio Mater* 2020;3:6400–7. doi: <https://doi.org/10.1021/acsabm.0c00837>.
- [14] Zielonka J, Joseph J, Sikora A, Hardy M, Ouari O, Vasquez-Vivar J, et al. Mitochondria-Targeted Triphenylphosphonium-Based Compounds: Syntheses, Mechanisms of Action, and Therapeutic and Diagnostic Applications. *Chem Rev* 2017;117:10043–120. doi: <https://doi.org/10.1021/acs.chemrev.7b00042>.
- [15] Broome SC, Woodhead JST, Merry TL. Mitochondria-targeted antioxidants and skeletal muscle function. *Antioxidants* 2018;7:107. doi: <https://doi.org/10.3390/antiox7080107>.
- [16] Khalilova LS, Nazarov PA, Sumbatyan NV, Korshunova GA, Rokitskaya TI, Dedukhova VI, et al. Uncoupling and toxic action of alkyltriphenylphosphonium cations on mitochondria and the bacterium *Bacillus subtilis* as a function of alkyl chain length. *Biochemistry (Mosc)* 2015;80:1589–97. doi: <https://doi.org/10.1134/S000629791512007X>.
- [17] Nazarov PA, Osterman IA, Tokarchuk AV, Karakozova MV, Korshunova GA, Yamzaev KG, et al. Mitochondria-targeted antioxidants as highly effective antibiotics. *Sci Rep* 2017;7:1394. doi: <https://doi.org/10.1038/s41598-017-00802-8>.
- [18] Teixeira J, Cagide F, Benfeito S, Soares P, Garrido J, Baldeiras I, et al. Development of a Mitochondriotropic Antioxidant Based on Caffeic Acid: Proof of Concept on Cellular and Mitochondrial Oxidative Stress Models. *J Med Chem* 2017;60:7084–98. doi: <https://doi.org/10.1021/acs.jmedchem.7b00741>.
- [19] Teixeira J, Oliveira C, Amorim R, Cagide F, Garrido J, Ribeiro JA, et al. Development of hydroxybenzoic-based platforms as a solution to deliver dietary antioxidants to mitochondria. *Sci Rep* 2017;7:6842. doi: <https://doi.org/10.1038/s41598-017-07272-y>.
- [20] Oliveira C, Cagide F, Teixeira J, Amorim R, Sequeira L, Mesiti F, et al. Hydroxybenzoic Acid Derivatives as Dual-Target Ligands: Mitochondriotropic Antioxidants and Cholinesterase Inhibitors. *Front Chem* 2018;6:126. doi: <https://doi.org/10.3389/fchem.2018.00126>.
- [21] Benfeito S, Oliveira C, Fernandes C, Cagide F, Teixeira J, Amorim R, et al. Fine-tuning the neuroprotective and blood-brain barrier permeability profile of multi-target agents designed to prevent progressive mitochondrial dysfunction. *Eur J Med Chem* 2019;167:525–45. doi: <https://doi.org/10.1016/j.ejmech.2019.01.055>.
- [22] Zhang JH, Chung TDY, Oldenburg KR. A simple statistical parameter for use in evaluation and validation of high throughput screening assays. *J Biomol Screen* 1999;4:67–73. doi: <https://doi.org/10.1177/108705719900400206>.
- [23] Clinical and Laboratory Standards Institute (CLSI). Methods for Dilution Antimicrobial Susceptibility Tests for Bacteria That Grow Aerobically; Approved Standard, in, CLSI standard M07, 2018.
- [24] Birmingham A, Seflors LM, Forster T, Wrobel D, Kennedy CJ, Shanks E, et al. Statistical methods for analysis of high-throughput RNA interference screens. *Nat Methods* 2009;6:569–75. doi: <https://doi.org/10.1038/nmeth.1351>.
- [25] Frei A, Zuegg J, Elliott AG, Baker M, Braese S, Brown C, et al. Metal complexes as a promising source for new antibiotics. *Chem Sci* 2020;11:2627–39. doi: <https://doi.org/10.1039/c9sc06460e>.
- [26] Abreu AC, Serra SC, Borges A, Saavedra MJ, Salgado AJ, Simões M. Evaluation of the best method to assess antibiotic potentiation by phytochemicals against *Staphylococcus aureus*. *Diagn Microbiol Infect Dis* 2014;79:125–34. doi: <https://doi.org/10.1016/j.diagmicrobio.2014.03.002>.
- [27] Borges A, Ferreira C, Saavedra MJ, Simões M. Antibacterial activity and mode of action of ferulic and gallic acids against pathogenic bacteria. *Microb Drug Resist* 2013;19:256–65. doi: <https://doi.org/10.1089/mdr.2012.0244>.
- [28] Blaskovich MAT, Zuegg J, Elliott AG, Cooper MA. Helping Chemists Discover New Antibiotics. *ACS Infect Dis* 2016;1:285–7. doi: <https://doi.org/10.1021/acsinfecdis.5b00044>.
- [29] Bolton JL, Dunlap T. Formation and Biological Targets of Quinones: Cytotoxic versus Cytoprotective Effects. *Chem Res Toxicol* 2017;30:13–37. doi: <https://doi.org/10.1021/acs.chemrestox.6b00256>.
- [30] Trnka J, Elkafal M, Anděl M. Lipophilic triphenylphosphonium cations inhibit mitochondrial electron transport chain and induce mitochondrial proton leak. *PLoS One* 2015;10:e0121837. doi: <https://doi.org/10.1371/journal.pone.0121837>.
- [31] Abreu AC, Serra SC, Borges A, Saavedra MJ, McBain AJ, Salgado AJ, et al. Combinatorial activity of flavonoids with antibiotics against drug-resistant *Staphylococcus aureus*. *Microb Drug Resist* 2015;21:600–9. doi: <https://doi.org/10.1089/mdr.2014.0252>.
- [32] Rajagopal M, Walker S. Envelope Structures of Gram-Positive Bacteria. *Curr Top Microbiol Immunol* 2017;404:1–44. doi: https://doi.org/10.1007/82_2015_5021.
- [33] Sutton JAF, Carnell OT, Lafage L, Gray J, Biboy J, Gibson JF, et al. *Staphylococcus aureus* cell wall structure and dynamics during host-pathogen interaction. *PLoS Pathog* 2021;17:e1009468. doi: <https://doi.org/10.1371/journal.ppat.1009468>.
- [34] Ahimou F, Denis FA, Touhami A, Dufrene YF. Probing Microbial Cell Surface Charges by Atomic Force Microscopy. *Langmuir* 2002;18:9937–41. doi: <https://doi.org/10.1021/la026273k>.
- [35] Malanovic N, Lohner K. Gram-positive bacterial cell envelopes: The impact on the activity of antimicrobial peptides. *Biochim Biophys Acta* 1858;2016:936–46. doi: <https://doi.org/10.1016/j.bbame.2015.11.004>.
- [36] Campos FM, Couto JA, Figueiredo AR, Tóth IV, Rangel AO, Hogg TA. Cell membrane damage induced by phenolic acids on wine lactic acid bacteria. *Int J Food Microbiol* 2009;135:144–51. doi: <https://doi.org/10.1016/j.ijfoodmicro.2009.07.031>.
- [37] Ota A, Abramovič H, Abram V, N. Poklar Ulrih, Interactions of p-coumaric, caffeic and ferulic acids and their styrenes with model lipid membranes. *Food Chem* 2011;125:1256–61. doi: <https://doi.org/10.1016/j.foodchem.2010.10.054>.
- [38] Tamba Y, Ohba S, Kubota M, Yoshioka H, Yoshioka H, Yamazaki M. Single GUV method reveals interaction of tea catechin (-)-epigallocatechin gallate with lipid membranes. *Biophys J* 2007;92:3178–94. doi: <https://doi.org/10.1529/biophysj.106.097105>.
- [39] Pérez-Peinado C, Dias SA, Domingues MM, Benfield AH, Freire JM, Rádís-Baptista G, et al. Mechanisms of bacterial membrane permeabilization by crotalidain (Ctn) and its fragment Ctn(15–34), antimicrobial peptides from rattlesnake venom. *J Biol Chem* 2018;293:1536–49. doi: <https://doi.org/10.1074/jbc.RA117.000125>.
- [40] Lambert PA, Hammond SM. Potassium fluxes, first indications of membrane damage in micro-organisms. *Biochem Biophys Res Commun* 1973;54:796–9. doi: [https://doi.org/10.1016/0006-291X\(73\)91494-0](https://doi.org/10.1016/0006-291X(73)91494-0).
- [41] Deus CM, Pereira SP, Cunha-Oliveira T, Teixeira J, Simões RF, Cagide F, et al. A mitochondria-targeted caffeic acid derivative reverts cellular and mitochondrial defects in human skin fibroblasts from male sporadic Parkinson's disease patients. *Redox Biol* 2021;45. doi: <https://doi.org/10.1016/j.redox.2021.102037>.
- [42] Amorim R, Cagide F, Tavares LC, Simões RF, Soares P, Benfeito S, et al. Mitochondriotropic antioxidant based on caffeic acid AntiOxClN4 activates Nrf2-dependent antioxidant defenses and quality control mechanisms to antagonize oxidative stress-induced cell damage. *Free Rad Biol Med* 2022;179:119–32. doi: <https://doi.org/10.1016/j.freeradbiomed.2021.12.304>.
- [43] Antonenko YN, Denisov SS, Khalilova LS, Nazarov PA, Rokitskaya T, Tashlitsky VN, et al. Alkyl-substituted phenylamino derivatives of 7-nitrobenz-2-oxa-1,3-diazole as uncouplers of oxidative phosphorylation and antibacterial agents: involvement of membrane proteins in the uncoupling action. *Biochim Biophys Acta Biomembr* 1859;2017:377–87. doi: <https://doi.org/10.1016/j.bbame.2016.12.014>.
- [44] Silva FAM, Borges F, Guimaraes C, Lima JLFC, Matos C, Reis S. Phenolic acids and derivatives: Studies on the relationship among structure, radical scavenging activity, and physicochemical parameters. *J Agric Food Chem* 2000;48:2122–6. doi: <https://doi.org/10.1021/jf9913110>.
- [45] Borges F, Guimaraes C, Lima JLFC, Pinto I, Reis S. Potentiometric studies on the complexation of copper(II) by phenolic acids as discrete ligand models of humic substances. *Talanta* 2005;66:670–3. doi: <https://doi.org/10.1016/j.talanta.2004.12.012>.
- [46] Hards K, McMillan DGG, Schurig-Briccio LA, Gennis RB, Lill H, Bald D, et al. Ionophoric effects of the antitubercular drug bedaquiline. *Proc Natl Acad Sci USA* 2018;115:7326–31. doi: <https://doi.org/10.1073/pnas.1803723115>.